

MICROCOPY RESOLUTION TEST CHART
NATIONAL BUREAU OF STANDARDS-1963-A

AD-A153 460



TECHNICAL REPORT RE-84-12

APPLICATIONS OF MODERN SPECTRAL ESTIMATION
TECHNIQUES TO RADAR DATA

Neal B. Lawrence
Ron C. Houts
Advanced Sensors Directorate
US Army Missile Laboratory

MARCH 1984



U.S. ARMY MISSILE COMMAND

Redstone Arsenal, Alabama 35809-5000

Approved for public release; distribution unlimited.

DTIC FILE COPY

DTIC
ELECTE
MAY 9 1985
B

DISPOSITION INSTRUCTIONS

DESTROY THIS REPORT WHEN IT IS NO LONGER NEEDED. DO NOT RETURN IT TO THE ORIGINATOR.

DISCLAIMER

THE FINDINGS IN THIS REPORT ARE NOT TO BE CONSTRUED AS AN OFFICIAL DEPARTMENT OF THE ARMY POSITION UNLESS SO DESIGNATED BY OTHER AUTHORIZED DOCUMENTS.

TRADE NAMES

USE OF TRADE NAMES OR MANUFACTURERS IN THIS REPORT DOES NOT CONSTITUTE AN OFFICIAL INDORSEMENT OR APPROVAL OF THE USE OF SUCH COMMERCIAL HARDWARE OR SOFTWARE.

DISCLAIMER NOTICE

THIS DOCUMENT IS BEST QUALITY PRACTICABLE. THE COPY FURNISHED TO DTIC CONTAINED A SIGNIFICANT NUMBER OF PAGES WHICH DO NOT REPRODUCE LEGIBLY.

REPORT DOCUMENTATION PAGE		READ INSTRUCTIONS BEFORE COMPLETING FORM
1. REPORT NUMBER RE-84-12	2. GOVT ACCESSION NO. AD-A153460	3. RECIPIENT'S CATALOG NUMBER
4. TITLE (and Subtitle) Applications of Modern Spectral Estimation Techniques to Radar Data		5. TYPE OF REPORT & PERIOD COVERED Technical Report
		6. PERFORMING ORG. REPORT NUMBER
7. AUTHOR(s) Neal B. Lawrence & Ron C. Houts		8. CONTRACT OR GRANT NUMBER(s)
9. PERFORMING ORGANIZATION NAME AND ADDRESS Commander, US Army Missile Command ATTN: AMSMI-RE Redstone Arsenal, AL 35898-5253		10. PROGRAM ELEMENT, PROJECT, TASK AREA & WORK UNIT NUMBERS
11. CONTROLLING OFFICE NAME AND ADDRESS Commander, US Army Missile Command ATTN: AMSMI-RE Redstone Arsenal, AL 35898-5253		12. REPORT DATE March 1984
		13. NUMBER OF PAGES 49
14. MONITORING AGENCY NAME & ADDRESS (if different from Controlling Office)		15. SECURITY CLASS. (of this report) Unclassified
		15a. DECLASSIFICATION/DOWNGRADING SCHEDULE
16. DISTRIBUTION STATEMENT (of this Report) Approved for public release; distribution unlimited.		
17. DISTRIBUTION STATEMENT (of the abstract entered in Block 20, if different from Report)		
18. SUPPLEMENTARY NOTES		
19. KEY WORDS (Continue on reverse side if necessary and identify by block number) Modern Spectral Analysis Adaptive Clutter Filtering Radar Adaptive Doppler Filtering Signal Processing Prediction Error Filter Maximum Entropy Least-Squares Spectral Estimation		
20. ABSTRACT (Continue on reverse side if necessary and identify by block number) The Modern Spectral Analysis (MSA) techniques involving linear prediction theory are reviewed and applied to radar signal processing. Specifically, the maximum entropy or forward-backward linear prediction method as implemented with Andersen's Burg algorithm is compared with the least-squares method as implemented with Marple's algorithm using as test signals autoregressive (AR) processes of 2nd and 4th orders plus single and dual sinusoids in Gaussian white noise. It is shown that Marple's indicators for terminating the AR model order iteration perform better than the more commonly employed Akaike or Parzen techniques for		

both AR processes and noisy sinusoids. The concept is examined for using MSA to predict the AR coefficients of a clutter-dominated radar return, and in turn employing these coefficients as a FIR digital filter to suppress the clutter. Recent work on adaptive clutter filtering is reviewed. The ability of these two algorithms to resolve two closely-spaced sinusoids in a high noise environment is studied using Tranter's test signal. It is shown that model-order size rather than signal-to-noise (SNR) seems to be the dominant factor for SNR in the range of 10 to 30 dB.

CONTENTS

	<u>Page</u>
I. OVERVIEW	1
II. MODERN SPECTRAL ESTIMATION TECHNIQUES	2
A. Yule-Walker Equations (YWE)	3
B. Maximum Entropy Special Estimation (MESE)	4
C. Estimating the AR Parameters	4
D. Forward-Backward Linear Prediction (FBLP).....	5
E. Least-Squares Spectral Estimation (LSSE)	6
F. AR Parameter Estimation for Long Data Records	7
G. AR Model Order Selection	7
H. Compensating Observation Noise	8
I. Computing R^{-1} from LPF Coefficients	8
III. CLUTTER SUPPRESSION	9
A. Clutter Spectral Estimation	10
B. Adaptive Doppler Signal Processor	11
C. Adaptive Lattice PEF	13
IV. SPECTRAL ESTIMATOR PERFORMANCE	15
A. AR Model Estimators	16
B. Noisy Sinusoid Estimation	18
C. Closely-Spaced Sinusoids Estimation	20
D. Target Identification	25
V. RESULTS AND RECOMMENDATIONS.....	26
REFERENCES	27
ACRONYM LIST	32
APPENDIX	35

LIST OF FIGURES

<u>Figure</u>	<u>Title</u>	<u>Page</u>
1	Lattice PEF	5
2	AR(2) Spectral Estimates using MLSA	16
3	AR(2) Spectral Estimates using ABA	17
4	AR(4) Spectral Estimates using MLSA	18
5	Double Sinusoid Spectral Estimate using ABA	23
6	Tranter's Test Case using MLSA	24
A-1	Computer Program for MSA	A-2
A-2	Example Printouts for AR(4) Process	A-7
A-3	Example Printouts for Noisy Sinusoid	A-8
A-4	PSD Plots for Noisy Sinusoid	A-11

I. OVERVIEW

The title of the work reported herein is quite similar to that used for the investigator's previous Battelle report [1]. Indeed, if the word "modern" were omitted they would be identical. Since that report was prepared, Kay & Marple [2] have written a comprehensive tutorial paper, "Spectrum analysis - a modern perspective," thoroughly outlining in 40 pages this topic which has so many potential application areas to military radar signal processing, e.g., array processing, clutter suppression, and target identification. It is pointed out in the literature [3] that the former two topics are basically spatial and spectral variations of the same problem, namely to solve

$$RA = X \quad (1)$$

for a set of variables (the vector A) given some known information about the signal (the autocorrelation matrix R) and some desired characteristics (the vector X). Kay & Marple's paper also includes 278 references, many of which have been incorporated into this report.

The basic interest in Modern Spectral Analysis (MSA) has centered on its superresolution feature, i.e., the ability to resolve two closely-spaced sinusoids. By closely-spaced, one implies a frequency separation less than $1/NT$, where N is the number of samples and T is the sampling interval, which is the accepted resolving capability of the N-pt. Discrete Fourier Transform (DFT). This claim to superresolution has been attacked by Rihaczek [4] who observed that the detailed target information required is lacking due to noise or clutter. In a rebuttal Jackson [5] pointed out that considerable progress had been recently made, citing among other things Marple's algorithm [6] which both significantly reduces the frequency estimation errors associated with Andersen's Burg-algorithm [7] for a low Signal-to-Noise Ratio (SNR) and virtually eliminates the spectral-line splitting associated with a high SNR. Indeed, in 1979 Tranter [8] observed many of these original deficiencies and in a later study [9] virtually wrote off this particular MSA technique because of noise problems. This author in last years report made a similar snap judgement based on Tranter's reports which stated that a SNR of at least 55 dB (later reduced by Shumway [10] to 40 dB) was required to resolve two closely-spaced sinusoids. It turns out that the problem lies in the technique used to estimate the order of the prediction filter, and that it works for a SNR as low as 20 dB, provided the prediction order is increased. Based on the widespread interest in MSA throughout the signal processing community, the U.S. Army would be well advised to continue monitoring progress in this area for potential applications.

This report contains a brief overview in Section II emphasizing the Least Squares Spectral Estimation (LSEE) technique associated with the m^{th} -Order Autoregressive (AR(m)) process. Section III deals with the application of MSA to the design of a Prediction Error Filter (PEF) to suppress clutter. Ironically the presence of clutter is one reason given by Rihaczek for rejecting MSA techniques. Section IV presents spectral estimation examples for AR(m) processes and noisy sinusoids generated from a computer program which is described in the Appendix. Some results and recommendations based on this study and the work reported in the literature are recorded in Section V.

II. MODERN SPECTRAL ESTIMATION TECHNIQUES

The basic problem is to estimate the power spectrum of a set of N samples $\{x(k)\}$. The development outlined in this section is a summary of the material found in Kay and Marple's tutorial [2] and is by necessity kept brief. The most general linear model is the Autoregressive Moving Average (ARMA) model described by the linear m^{th} -order difference equation

$$x(n) = \sum_{i=0}^m b(i)w(n-i) - \sum_{k=1}^m a(k)x(n-k) \quad (2)$$

In digital filter terminology, a Linear Prediction Filter (LPF) is defined by $\{w(n)\}$ as the input sequence, $\{x(n)\}$ as the output sequence, with $\{b(i)\}$ the feed-forward coefficients (FIR filter), and $\{a(k)\}$ the feed-back coefficients (FIR filter). The system function $H(Z)$ is obtained by taking the Z-transform of Eqn. (2) and solving for the ratio $X(Z)/H(Z)$.

$$H(Z) = \frac{\sum_{i=0}^m b(i)Z^{-i}}{\sum_{k=0}^m a(k)Z^{-k}}, \quad (3)$$

where $a(0) \triangleq 1$ and some $b(i)$ or $a(k)$ can be zero subject to the constraint $a(m) \neq 0$, i.e., the filter is of order m , denoted $O(m)$. The power spectral density (PSD) of the output is given by

$$I_x(Z) = |H(Z)|^2 P_n(Z) \quad (4)$$

where $P_n(Z) = \sigma^2 T$ if the input sequence consists of samples every T_s from a white noise process of zero mean and variance σ^2 . The PSD as a function of frequency is obtained from Eqn. (4) by replacing $Z \rightarrow \exp(j2\pi fT)$ where f is a continuous frequency measured in Hertz (Hz).

The general ARMA model can be decomposed into two simpler models, namely Moving Average (all $a(k) = 0$, except $a(0) = 1$) and Autoregressive (all $b(i) = 0$, except $b(0) = 1$) which by Eqn. (3) can also be termed the all-zero and all-pole models, respectively. The autoregressive (AR) model is the subject of primary interest in this study. It follows from Eqn. (4), assuming white noise input, that the AR PSD is

$$P(f) = \frac{\sigma^2 T}{1 + \sum_{k=1}^m a(k) \exp(-j2\pi f k T)}^2 \quad (5)$$

The numerator is a scale factor; consequently, the relative PSD is completely determined by knowledge of the parameter set $\{a_m(k)\}$ of the AR process of order m , $AR(m)$, with the understandings that the parameter subscript m can be dropped whenever obvious and $a_m(0) = 1$ for all m . Furthermore, the final value in each set is known in the literature as the reflection coefficient (K_m), i.e.,

$$K_m = a_m(m) \quad (6)$$

The FIR digital filter with weights $\{a_m(k)\}$, $x(n)$ as input and $w(n)$ as output is called a Prediction Error Filter (PEF). The obvious question remains, given a sample set $\{x(k)\}$ how does one obtain $\{a(k)\}$ in order to determine $P(f)$ from Eqn. (5).

A. Yule-Walker Equations (YWE)

The original developments for finding the $\{a(k)\}$ for the M^{th} -order LPF assumed knowledge of the autocorrelation values, which in theory are given by

$$R(k) = E\{x(n+k)x^*(n)\} \quad (7)$$

where $E\{ \}$ implies statistical expectation and the superscript (*) complex conjugation. The YWE

$$R(k) = \begin{cases} - \sum_{i=1}^M a(i)R(k-i) & k > 0 \\ - \sum_{i=1}^M a(i)R(-i) + \sigma^2 & k = 0 \end{cases} \quad (8)$$

follow by substituting Eqn. (2) into Eqn. (7) and recognizing that $E\{x(n+k)x^*(n)\}$ is non zero ($=\sigma^2$) only for $k=0$. The AR parameter set is obtained by selecting M equations from the semi-infinite set of Eqn. (2) and solving for σ^2 from the $k=0$ equation. In matrix form this is

$$[R(i-k)]_{(M,M)} \times [a(i)]_{(M,1)} = - [R(1)]_{(M,1)} \quad (9)$$

where subscript (x,y) implies a matrix of x rows and y columns. The matrix $[R(i-k)]$ is Hermitian and Toeplitz i.e., $R(i,k) = R(i-k) = R^*(k-i)$. Rearranging Eqn. (9) and including the row for σ^2 yields

$$\begin{aligned} [R(i-k)]_{(M+1,M+1)} [1 \ a(1) \ \dots \ a(M)]'_{(M+1,1)} \\ = [\sigma^2 \ 0 \ 0 \ \dots \ 0]'_{(M+1,1)} \end{aligned} \quad (10)$$

where prime (') implies a vector transpose. The YWE given by Eqn. (10) can be solved for $\{a(i)\}$ by inverting the matrix $[R(i-j)]$ provided the first $(M+1)$ -lags of the autocorrelation are known. Because of the Toeplitz structure, the standard matrix inversion, requiring $O(M^3)$ operations, can be replaced by the Levinson-Durbin Equation (LDE), which only require $O(M^2)$ operations. The technique is to recursively solve the AR(m) parameter set $\{a_m(k)\}$ for $m = 2, 3, \dots, M$ using the algorithm

$$a_m(m) \triangleq K_m = \sigma_{m-1}^{-2} [R(m) + \sum_{i=1}^{m-1} a_{m-1}(i) R(m-i)]$$

$$a_m(i) = a_{m-1}(i) + K_m a_{m-1}^*(m-i)$$
(11)

$$\sigma_m^2 = [1 - |K_m|^2] \sigma_{m-1}^2$$

subject to the initial conditions

$$K_1 = \frac{R(1)}{R(0)}$$
(12)

$$\sigma_1^2 = [1 - |K_1|^2] R(0).$$

Since the desired order (M) of the LPF is not known a priori, Eqn. (11) can be solved for successively higher-order values of m until the modeling error σ_m is reduced to an acceptable value. Further, since $|K_m| < 1$, it follows from Eqn. (11) that $\sigma_{m+1} < \sigma_m$; moreover, if the $\{x(k)\}$ are truly samples of an AR(M) process, the modeling error reaches an irreducible minimum σ_m . The poles of A(Z), the denominator of Eqn. (3), can be shown to lie within the unit circle, i.e., the LPF is stable, or marginally stable (poles on the unit circle) if the AR process consists only of sinusoids.

B. Maximum Entropy Spectral Estimation (MESE)

The concept of AR(m) modeling and associated LPF design has been shown to be equivalent to the Maximum Entropy Method (MEM) proposed originally by Burg [11, 12], provided the autocorrelation lags are known and the random process is Gaussian. Burg suggested that extrapolation of the m known correlation lags should be performed in such a manner that the corresponding time series has maximum entropy, i.e., the PSD should be as white as possible given the known lags. The MESE is given by Eqn. (5) with the $\{a(k)\}$ obtained from solution of Eqn. (10).

C. Estimating the AR Parameters

Unfortunately, in a radar system the $\{R(k)\}$ values are unknown and all one can begin with are the N time samples $\{x(k)\}$ from an assumed AR(m) process. Although one might estimate the desired correlation samples by the biased estimator.

$$\hat{R}(k) = \frac{1}{N} \sum_{n=1}^{N-k} x(n)x^*(n+k)$$
(13)

It has been shown for short data records ($N \leq 100$) the YWE produces poor spectral estimates.

FREQ. 0.11250000E+00 MAX. 0.0000000E+0

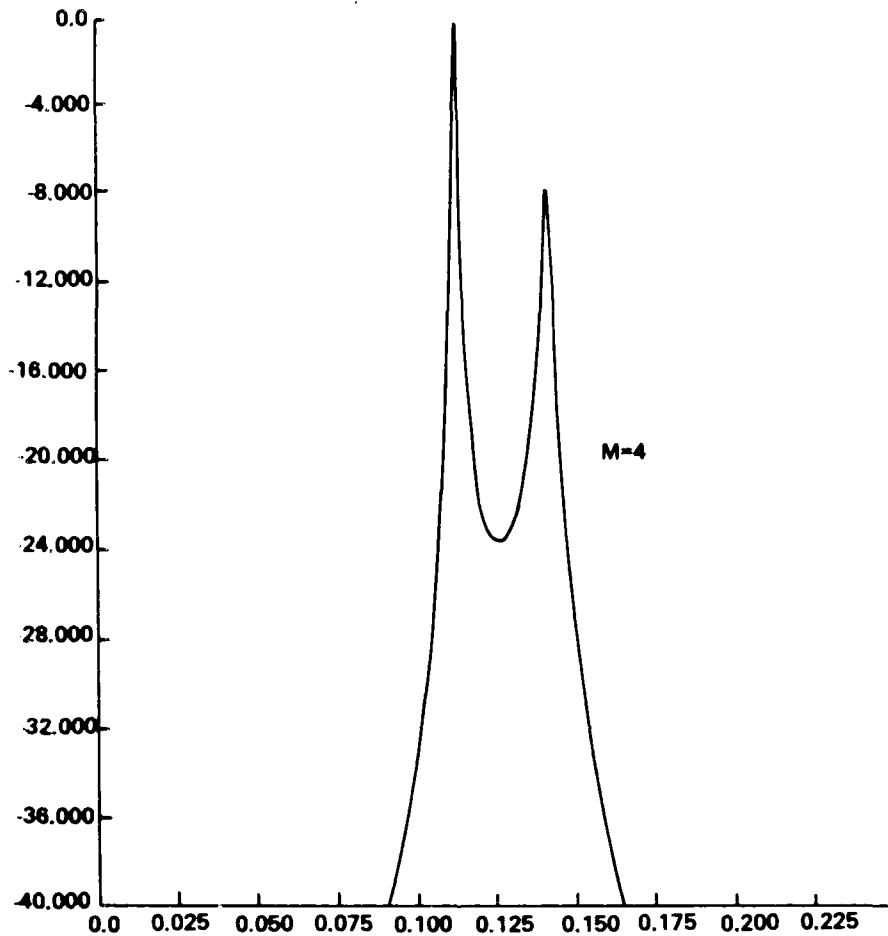


Figure 4. AR(4) spectral estimate using MLSA.

B. Noisy Sinusoid Estimation

The first problem to be examined is a noisy sinusoid given by

$$y(k) = A \cos(\theta k + \phi) + n(k) \quad (41)$$

where $\theta \triangleq 2\pi f_c T$ and $n(k)$ is a sample from a complex Gaussian process with zero mean and variance σ^2 in either the real or imaginary component. The SNR (not in dB) is given by

$$\alpha = A^2 / 2\sigma^2 \quad (42)$$

and is applicable for both real and complex data. Swingler showed [45] that the signal portion of Eqn. (41) when estimated by the ABA has a frequency estimate which differs from f_c by

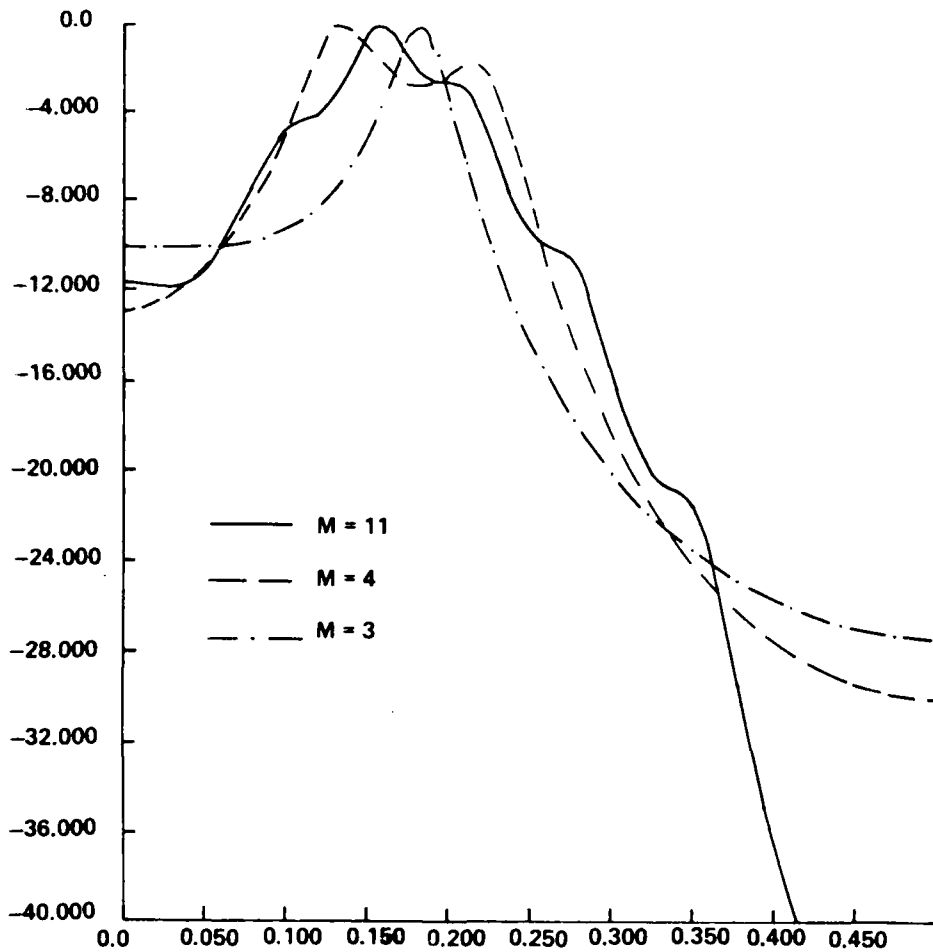


Figure 3. AR(2) spectral estimates using ABA.

The second example is a 40 sample AR(4) process with coefficients $\{2.7607, -3.8106, 2.6534, -0.9238\}$ and $\text{CNR} = 50$ dB. The spectral estimate which results from setting the maximum allowed order (MM) equal to four in the MLSA is shown in Figure 4. This spectrum is suggestive of that produced by broadband-type (bandlimited white noise) jamming and presumably could be suppressed in a fashion similar to clutter using a PEF. The algorithm terminated at $M=4$ because the ratio of final-to-initial prediction error energies was below $\text{TOL} = 0.001$. Essentially, an identical result for $M=4$ was obtained with the ABA; however, the three PEF-order indicators tabulated in Figure A-2 all predicted $M > 4$. Ulrych & Bishop observed that the histogram of absolute minimum FPE-order indicators obtained from 100 estimates of AR(2) and AR(4) processes was rather broad, but improved with significant numbers at $n=M$ if MM was restricted to $N/3$. They also determined that the histogram of first FPE minimum (vs. absolute minimum) was quite similar, an approach to selecting M which is commonly used.

A. AR Model Estimations

Two AR models specified by Ulrych & Bishop [15] for real data were used to verify the two algorithms and demonstrate the applicability of this technique to wideband spectral estimation. The first example was a 20 sample AR(2) process with coefficients $\{0.75, -0.50\}$ and $\text{CNR} = 50$ dB producing a theoretical spectrum which looks somewhat like weather clutter. The results obtained with MLSA for $M=3$ and $M=4$ are shown in Figure 2. The $M=3$ solution is obviously not a good estimate; however, the $M=4$ solution is essentially identical to that shown in Ulrych & Bishop. Results obtained from the ABA for $M=3, 4$ and 11 are shown in Figure 3. Obviously, the ABA does not produce as accurate a prediction. Moreover, the $M=11$ example shows the effect of overestimating M excessively. A change of N from 20 to 50 samples had no noticeable effect on the spectral estimates.

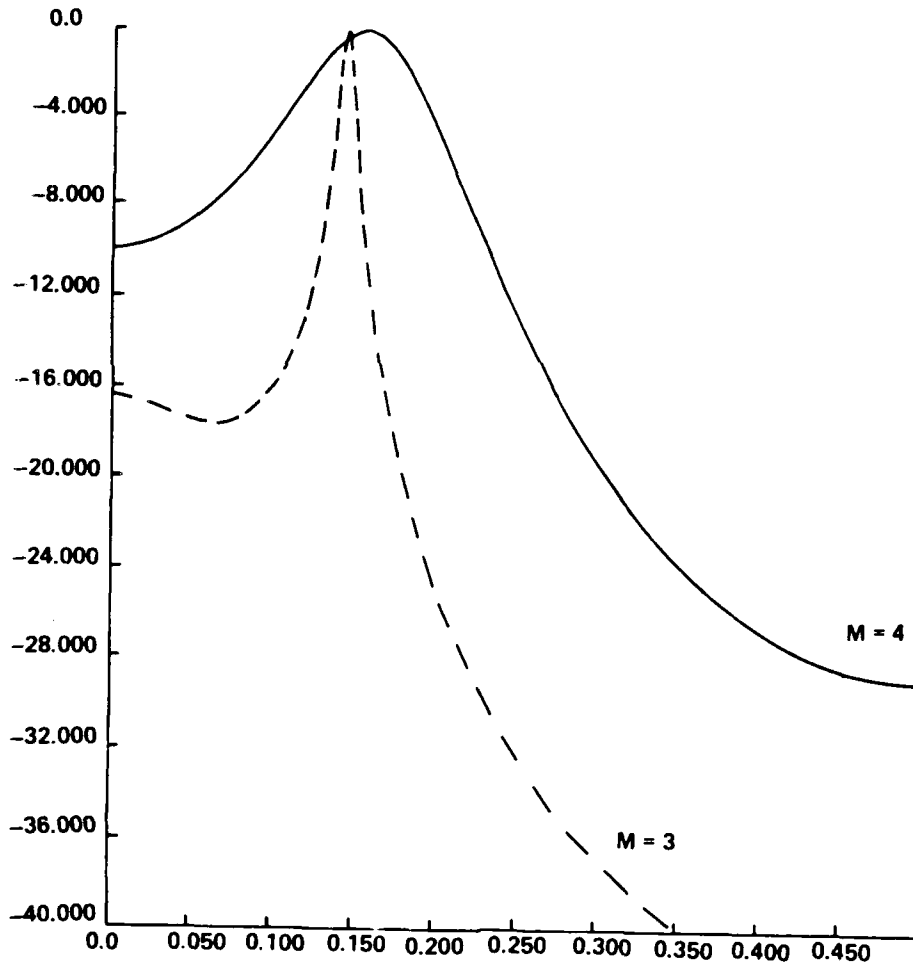


Figure 2. AR(2) spectral estimates using MLSA.

Gibson and Haykin observed that the number of sections required is at least equal to the number of spectral peaks, equal for sharp peaks, but typically two or three for each broad peak such as clutter produces. They demonstrated the adequacy of a notch filter ($M=1$) for a sinusoid and the effect of changing M for a Gaussian shaped clutter spectrum, see Eqn. (27). Increasing M from 1 to 3 essentially broadened the stopband to match the clutter bandwidth while additional stages did little except to flatten the passband gain. They also illustrated how to select t_1 when the clutter extent is $t_c = 100$ and signal duration $t_s = 20$. Initial clutter modeling showed that decoupling occurred when $t_1 = 25$ for $W = 0.9$. It follows from Eqn. (39) that $a = 2.64$, and from their second choice of $W = 0.95$ with signal and clutter present, that the new $t_1 = 51$ is consistent with setting $t_1 = t_c/M$ where a second-order ($M=2$) PEF was specified. A flow chart for implementing the recursive reflection coefficient computations for either method is provided [43].

In two conference papers Gibson, et. al., studied the adaptive lattice PEF using simulated [39] and actual [44] radar clutter data in complex form. The earlier paper (1979) with simulated data employed Method I and defined $W = 0.95$ and $M = 2$ based upon a large number of test cases. It was observed that W is a function of the number of clutter samples (N) with $W = 0.98$ for $N = 250$ vs. 0.95 for $N = 100$. Published filter responses were shown to be a function of CNR with little variation for $\text{CNR} \geq 10$ dB. When expressed in terms of SIR, the average enhancement exceeded 20 dB for "average storm" conditions and 16 dB for "serve storm" conditions. The latter reflects a situation where the conventional MTI would not properly suppress the clutter due to its increased bandwidth. The later paper (1981) tested the performance of the lattice PEF employing Method II using actual radar returns from stationary and nonstationary clutter with and without targets present. The improvement ratio (SCR-out over SCR-in for MTI or PEF) was always positive for the PEF, ranging from 2 to 8 dB, whereas the range was -17 to +16 dB for the MTI with poor performance associated with adverse weather conditions. The radar used employed pulse staggering with four unique interpulse spacings. In order to employ this data with the lattice filter, the signal returns were subdivided into four groups each having five target samples and 25 clutter returns. The subsets were filtered independently and the displayed graphs represented the average of the four subsets for input, MTI and lattice PEF outputs. The choice of adaptive weighting factor ($U=0.6$) and filter order ($M=5$) were determined only after extensive testing, probably required by the small number of samples ($N=20$) available.

IV. SPECTRAL ESTIMATOR PERFORMANCE

The maximum entropy and least squares spectral estimators were described in Section II and their applicability to clutter suppression in Section III. The purpose of this chapter is to present details regarding their applicability to the spectral estimation of AR(m) processes and noisy sinusoids, both single component and two sinusoids spaced closer than the DFT resolution width. The computer algorithms ABA and MLSA are used for the MESE and LSSE, respectively. A computer program which can generate noisy complex data samples and estimate the spectrum using either algorithm is described in the Appendix along with some typical examples.

exponentially weighted and eventually eliminated. Method II updates the crosspower (numerator) and autopower (denominator) expectations separately, which yields

$$K_{m+1}(n) = \frac{v_{m+1}(n)}{y_{m+1}(n)} \quad (36)$$

where

$$v_{m+1}(n) = U \cdot v_{m+1}(n-1) - 2f_m(n) \cdot b_m^*(n-1) \quad (37)$$

$$y_{m+1}(n) = U \cdot y_{m+1}(n-1) + |f_m(n)|^2 + |b_m(n-1)|^2$$

with U being the new adaptive weighting factor and $v_{m+1}(0) = y_{m+1}(0) = 0$. The forward-backward prediction errors were defined in Eqn. (15). Method II has the advantage of not assuming constant power and should work best with nonstationary signals. However, it is more complicated computationally and has a more complex convergence relationship. They also showed that Methods I and II were special cases of Griffiths' algorithm. It was further demonstrated that for Method II K_1 converged to its optimal value more rapidly with a corresponding faster decrease in $|f_1(n)|$. The problem of coefficient decoupling was also addressed and shown to be a significant consideration.

Decoupling is a problem because initially all $\{K_m\}$ in the M^{th} -order PEF adapt to the strongest spectral component. Eventually K_1 adapts properly and the remaining $M-1$ coefficients attack the next strongest component, etc. Furthermore, residual coupling remains after the major decoupling occurs, thus interfering to some extent with convergence properties of later stages. The first stage decoupling time (t_1) is proportional to \bar{n} , i.e.,

$$t_1 = a\bar{n} \quad (38)$$

where a is a dimensionless constant associated with a specific signal type. For method I, it follows from Eqn. (35) that

$$W = \exp(-a/t_1) \quad (39)$$

Unfortunately, a similar expression does not exist for the weighting factor U of Method II. Assuming the incoming signal consists of both clutter with duration t_c and signal with considerably smaller duration t_s , then

$$t_s < t_1 < t_c \quad (40)$$

As the filter order increases t_1 is set closer to t_s , and for very large t_c , the upper limit is typically divided by an integer ranging from one to M , thus insuring time for higher-order stages to converge.

rejected in favor of the original ABA because it required three times as many complex multiplications for this application. He also rejected Andersen's suggested modification [13], i.e., Eqn. (18) on the basis of sensitivity to computational errors. The current RADC system can process 128 range cells and allows 32 updates of the weight-vector components during this dwell time. Although currently operating with the Burg algorithm, the adaptive processor is reprogrammable. Documentation of the RADC system should be available shortly.

C. Adaptive Lattice PEF

Gibson and Haykin in a series of paper [39] show that clutter suppression can be achieved using an adaptive PEF with the lattice structure as opposed to the more conventional Tapped Delay Line (TDL) used to implement Eqn. (32). The lattice PEF structure was shown in Figure 1 and the recursion relations were given by Eqn. (15). Burg's (harmonic-mean) algorithm states that the optimum values of the reflection coefficients $\{K_m\}$ are given by the ratio of the expectations of the negative crosspower to the mean value of the two prediction error autopowers for that PEF stage (m). Makhoul [40] describes a variety of alternatives to the harmonic mean definition for calculating $\{K_m\}$, but concludes that Burg's is preferred "because it minimizes a reasonable and well-defined error criterion", a view supported by Gibson [41]. If adaptation were not required, i.e., the input signal was from a stationary process, the $\{K_m\}$ for Burg's algorithm are given by Eqn. (17).

When clutter is to be suppressed in either the presence or absence of a doppler-return signal, it follows that the PEF coefficients must be updated routinely, i.e., adapted to changes in the radar return. Griffiths [42] compares the lattice and TDL filters from the viewpoint of adaptive filtering and concludes that the lattice enjoys convergence advantages at the expense of increased computations. The lattice structure for stationary processes permits the independent optimization of each K_m , which carries over to some degree for the adaptive case. It is also possible to trade off adaptation rate and prediction error with filter length. Gibson and Haykin [43] studied the properties of adaptive lattice PEF and proposed two methods for recursive estimation of K_m on an incoming sample-by-sample basis. Method I adds a correction term to the previous value which yields

$$K_{m+1}(n) = W \cdot K_{m+1}(n-1) + A_m(n) \cdot f_m(n) \cdot b_m^*(n-1), \quad (34)$$

where $f_m(n)$ and $b_m(n)$ are given by Eqn. (15), and

$$A_m(n) = \frac{-2(1-W)}{|f_m(n)|^2 + |b_m(n-1)|^2} \quad (35)$$

with

$$W = \exp(-1/\bar{n}) \quad , \quad (36)$$

where \bar{n} is the length (in samples) required for the filter to adapt. The adaptive weighting factor (W) is designed to insure that old estimates are

Incorporating the adaptive whitening filter and the DFB in one step has been reported by Sawyers [38, 25]. The resulting coefficients are obtained from Eqn. (31) with R^{-1} obtained from Eqn. (25) using the MEM algorithm. The coefficient set obtained from N samples in one dwell is used to define the adaptive DFB coefficients for the next dwell in the same range cell. Should a target be detected in that cell, the update algorithm is inhibited so as not to suppress the target spectrum. Sawyers presents performance results for a pulse-doppler radar ($N = 32$, $M = 15$) using a simulated interference spectrum including ground, rain and broadband jamming with clutter-to-noise ratios of 50, 20, and 30 dB, respectively. The simulation assumes unit signal voltage and unit thermal noise power per returned pulse. Optimally, a SIR of 14.8 dB is possible for a particular doppler filter ($f_n T = 0.375$) with the actual design indicating 14.0 dB. The improvement is definitely a function of Doppler, as a second Doppler choice ($f_n T = 0.5625$) just below the broad-band jamming has an optimal SIR of 11.9 dB with the actual result some 2.5 dB less. It is suggested that additional dwell averaging be invoked in such cases, i.e., the reflection coefficient K_m given by Eqns. (17) and (18) becomes for D-dwell averaging

$$K_m = -2 \frac{\sum_{i=1}^D \text{Num}(i)}{\sum_{i=1}^D \text{Den}(i)} \quad (33)$$

where $\text{Den}(i)$ is defined by Eqn. (18) and $\text{Num}(i)$ is the summation expression in Eqn. (17). Only limited results were presented for actual radar data and no attempt was made to determine the SIR.

Nitzberg [23] reported an adaptive DFB, similar to Sawyers, designed by General Electric for the USAF Rome Air Development Center, (RADC). This system was implemented with the Burg algorithm and did a MESE for $N = 16$. It appears that the estimated clutter spectrum for one range cell was used to filter the clutter in the next cell as opposed to the same cell one dwell-time later. There was no discussion of dwell averaging to improve the estimated spectrum. Nitzberg did study the effects of a "Mismatch Loss" due to the AR(M) spectrum not matching the true spectrum by investigating the Clutter-to-Noise Ratio (CNR) after filtering vs. filter-order (M) for various input CNR. The simulated clutter had a Gaussian spectrum, from which the correlation matrix can be determined, hence the optimum weights from Eqn. (31) and residual CNR decreased to within a few dB of the theoretical optimum. How rapidly it converged to the optimum depended on the original CNR, e.g., if the input CNR is 35 dB the residual is 4 dB, whereas for 65 dB the residual is roughly 14 dB, which is some 10 dB above the optimum weight result. The mismatch loss is also shown to be dependent upon the normalized clutter standard deviation (σT) and the relative separation of the clutter mean from the doppler filter center frequency, increasing with the former and decreasing with the latter as they increase in value. Nitzberg also discussed an "Estimation Loss" due to the AR(M) parameters being estimated from data samples as opposed to known values of the R-matrix. He showed that the estimation loss tends to increase with the LPF order thus making it difficult to determine the optimum order. The more recent Marple algorithm [6] was

B. Adaptive Doppler Signal Processor

Other researchers [3, 34, 35] had proposed designing filters to maximize the Signal-to-Clutter Ratio (SCR) as opposed to the conventional match filter, which maximizes the SNR, where the noise is assumed to be white Gaussian. The problem was that the clutter characteristics had to be specified a priori. Two examples where this philosophy was employed were the Hughes' Aircraft Co. designs of a Doppler Filter Bank (DFB) for the TPQ-37 artillery locator [36] and the U. S. Army Missile Command's Quiet Radar. Basically, a conventional matched filter can be implemented for a given Doppler shift (f_n) using a Discrete Fourier Transform (DFT), whereas a filter matched to a specified Signal-to-Interference Ratio (SIR) is obtained by maximizing

$$\text{SIR} = \frac{(\underline{w}^\dagger \underline{s})^2}{\underline{w}^\dagger R \underline{w}} \quad (29)$$

Assuming uniform transmit weights, \underline{s} is a steering vector defined by

$$\underline{s}(n)^\dagger = [\exp(-j\pi(N-1)f_n T), \exp(-j\pi(N-3)f_n T), \dots, \exp(+j\pi(N-1)f_n T)], \quad (30)$$

and R is the $N \times N$ matrix of correlation samples. The vector of filter coefficients \underline{w} can be obtained by solving

$$\underline{w}(n) = R^{-1} \underline{s}(n) \quad , \quad (31)$$

where the "n" is identified with the Doppler frequency f_n . The solution of Eqn. (31) depends on finding R^{-1} , which was discussed previously in Section II.1. Such an inverse technique has a computational complexity of $O(N)$ to $O(N^2)$ as opposed to direct inversion by Gaussian elimination of $O(N^3)$. Another technique for estimating R^{-1} involves Kalman filtering which has a computational complexity $O(N^2)$. This approach was used by Bowyer et al [37] in designing an adaptive clutter filter for a problem involving ballistic missiles where booster-tank break up upon atmospheric reentry caused a false target. They observed that their Kalman estimator approach was far superior to the earlier FIR filters which used feedback to adjust the weights and had a long convergence time on the order of NT ($20 < N < 30$). Their technique assumed an AR(M) clutter model ($2 \leq M \leq 4$) with the spectral coefficients $\{\hat{a}(i)\}$ obtained from the Kalman filter used to construct a whitening filter

$$H_w(Z) = 1 - \sum_{i=1}^M \hat{a}(i) Z^{-i} \quad , \quad (32)$$

whose structure can be readily changed with the clutter. The entire N samples were then whitened and sent to a conventional matched filter with coefficients adjusted to reflect signal whitening. No attempt was made to integrate the whitening process with the DFB. It was also pointed out that the estimator memory is a drawback to using the Kalman filter algorithm. Consequently, if the clutter is not extended in time, the estimates do not change rapidly and it becomes necessary to introduce some mechanism such as exponentially fading memory to insure proper adjustment.

which can be approximated [27] with an error $|\epsilon| < 2.7 \times 10^{-3}$ by

$$P_g(F) = [C(0) + C(2)F^2 + C(4)F^4 + C(6)F^6]^{-1}, \quad (28)$$

with $\{C(n)\} = \{2.490895, 1.466003, -0.024393, 0.178257\}$. It should be noted that F represents the actual frequency normalized with respect to a parameter which depends both upon the transmit frequency and the nature of the clutter. The important point is that both forms can be considered as all-pole functions and hence modeled as AR(M) processes where M is $n/2$ for the Butterworth model (typically $2 \leq n \leq 4$) and three (3) for the Gaussian-approximation model of Eqn. (28). Since n in Eqn. (26) is not required to be an integer and the Gaussian model is an approximation, a realistic M -value would be somewhat larger. Obviously, larger M -values imply more computation and peaky spectral approximations.

Hawkes and Haykin [28] developed a computer model for I&O channel (complex-data) clutter samples which assumes a large number of elemental dipole scatters arranged in a two-dimensional (range and azimuth) array. The model included Probability Density Functions (PDFs) to describe the dipole rotation frequency, doppler shift due to clutter, and a factor to describe the antenna pattern.

A. Clutter Spectral Estimation

Kesler and Haykin [29, 30] used Burg's MEM technique to estimate the clutter PSD. The aforementioned computer data was used assuming a steady dipole frequency and describing the doppler variations by a Gaussian PDF of zero-mean and standard deviation σ . Akaike's FPE algorithm was used to determine the appropriate choice for M . They also generated samples of AR(2) and AR(4) processes (real-valued) which yielded rather poor MESE, looking neither like the theoretical curves or each other as M was varied above and below the FPE estimate. However, when complex data was used, either from the computer model or an AR process, the resulting spectra were relatively insensitive to the choice of M or N . It should be observed that N was typically quite large (≥ 64) for the AR process and that the results were sensitive to start-up effects, i.e., the number of AR-model samples ignored. However, the computer-model data results looked similar to the theoretical spectrum for N as low as 16. By comparison spectra obtained by applying Welch's periodogram method (Fourier analysis) to the same data yielded unacceptably broad spectra for $N \leq 64$. In later papers [31, 32] the MEM approach was applied to true radar clutter (complex data) including ground, weather and birds. The ground and weather clutter spectra were quite insensitive to N provided it was in the range 10 to 30 samples or greater. The bird-spectra were quite variable with N in agreement with variable spatial and temporal distributions within flocks. Their conclusions were that good MESE could be obtained for a particular range bin using only one look. They also suggested that MEM might be used for on-line classification of various clutter sources. Hawkes and Haykin in an earlier paper [33] had proposed an adaptive Moving Target Indicator (MTI) the coefficients of which were chosen based on a decision as to what type of clutter was encountered. This decision was based on applying the autocorrelation of the incoming signal to a decision algorithm and comparing the output against a set of precomputed clutter characteristics.

where (\dagger) implies a complex-conjugate transpose operation. The inverse matrix is both Hermitian ($R^{-1} = (R^{-1})^\dagger$) and persymmetric (symmetric about both diagonal directions). The matrix A is $N \times N$ with the first $N - M$ columns consisting of $\{a_m(k)\}$ with $\{0, 1, 2, \dots, (N-M)\}$ leading zeros and $\{(N-M-1), \dots, 2, 1\}$ trailing zeros respectively, plus M columns consisting of $\{a_m(k)\}$, $m = 0 \rightarrow M$ arranged with the proper number of leading zeros ($N-M$ for $m=M$ up to $N-1$ for $m=0$). The matrix D is an $N \times N$ diagonal matrix with $1/E_M$ for the first $N-M$ diagonal elements and $\{1/E_{M-1}, \dots, 1/E_1, 1/E_0\}$ for the remaining M elements. Details regarding the derivation of Eqn. (24) beginning with the YWE are also found in Herring [22]. Nitzberg [23] observed that it should be possible to compute R^{-1} using only the PEF set for $m=M$ and suggested a technique for complex-data based on Siddiqui [24]. Although Nitzberg's algorithm was not published, Sawyers [25] independently presented such a solution assuming $M \leq N/2$ and showed that $\{Z(i,j)\}$ the elements of R^{-1} are given by

$$Z(i,j) = a(i-1)a^*(j-1) + Z(i-1,j-1) \quad (25a)$$

where $i = 1, 2, \dots, \min(N/2, M+1)$ and $j = i, i+1, \dots, M+1$; or

$$Z(i,j) = Z(i-1,j-1) \quad (25b)$$

for $i = 2, 3, \dots, \min(N/2, M+1)$ and $j = M+2, M+3, \dots$, provided $N \geq 2(M+2)$, also for $i = M+2, M+3, \dots, N/2$ and $j = i, i+1, \dots, i+M$; or

$$Z(i,j) = 0 \quad (25c)$$

for $i = 1, 2, \dots, N/2$ and $j = i+1+M, i+2+M, \dots, N$; or

$$Z(j,i) = Z^*(i,j) \quad (25d)$$

for $i = 1, 2, \dots, N/2-1$ and $j = i+1, i+2, \dots, N/2$. The elements of the lowerhalf of R^{-1} could be obtained from the fact that R^{-1} is Hermitian and persymmetric. In reality, the upper-half of R^{-1} is sufficient for the clutter application described in Section III.

III. CLUTTER SUPPRESSION

Clutter is a general term describing radar returns from objects other than targets of interest e.g., ground, rain clouds, or bird reflections. It does not include energy received from deliberate attempts to interfere with radar performance such as chaff or active jamming. Zehner and Currie in a recent study [26] suggest that the best PSD models are Butterworth

$$P_b(F) = \frac{A}{1+F^n} \quad (26)$$

and Gaussian

$$P_g(F) = \frac{1}{\sqrt{2\pi}} \exp(-F^2/2), \quad (27)$$

Inspection of Eqns. (22) and (23) show that a penalty is paid for selecting $m > M$, since E_m decreases slower than the compensating factor or term increases. Ulrych and Bishop [16] have studied the Akaike FPE criterion for both YWE and ABA. Histograms of the minimum FPE location for 100 realizations of AR(2), (N=20) and AR(4), (N=40) data sets indicated peaks when $m=M$ and $m=N$. When the order was constrained ($m \leq N/3$) a single peak near $m=M$ occurred. Their studies, supported later by Jones [17], indicated that with $m \leq N/2$ the first minimum in Eqn. (22) should be used to determine the LPF order for an AR(M) process. If the data comes from noisy sinusoids a clear minimum for the FPE does not exist, and the first local minimum could easily produce a poor spectral estimate. Landers and Lacoss [18] studies all three order-predictors which showed that the CAT technique produced a sharp minimum for noise-free sinusoids when compared to the Akaike methods. However, there was little distinction among the three for the same sinusoid plus 50% uniform noise. It did appear that a single minima occurred in predictor-algorithm vs. order-selected plots when processing a complex sinusoid as contrasted with either the real or imaginary components. Unfortunately, it is often the size and location of narrowband spectral components which are of interest, whereas, the order-predictor algorithms are based upon the entire spectrum including any noise present.

H. Compensating Observation Noise

When observation noise is added to samples of an AR process, the result is really an ARMA process and spectral estimates derived from LSSE and MESE are inaccurate, becoming worse as the Signal-to-Noise Ratio (SNR) decreases. Unfortunately, ARMA modeling techniques are not well developed, particularly for short data records [2, p. 1397]. A second approach is to use the AR modeling but let $m = N/3$. Kay [19] has shown that it is possible to detect a noisy sinusoid (SNR = 0dB) with $m=32$ (N=100). In a subsequent paper [20] Kay investigated a second approach, namely compensating the R-matrix directly by subtracting $\alpha \sigma_n^2 I$, where α is a decimal fraction of the observation noise power (σ_n^2) and I is the identity matrix i.e., ones only on the principal diagonal. Unfortunately, one does not know how much noise to remove. Tranter [9] has studied this technique for the cases of one or two real-valued noisy sinusoids. The Pisarenko Harmonic Decomposition (PHD) technique is a special case which will be examined subsequently in Section IV. It does not assume that the sinusoids are harmonically related and is a special ARMA process which has equal AR and moving-average parameters.

I. Computing R^{-1} from LPF Coefficients

Although the PSD of the AR(M) process can be determined directly from the LPF coefficient set $\{a_M(k)\}$, i.e., without ever generating the actual correlation matrix R; there are practical reasons for needing R-inverse (R^{-1}). Burg addressed this point in his 1968 paper [12] and Andersen [7] gave a general solution in terms of the PEF sets and prediction errors (P_m) for orders $m = 0 \rightarrow M$. Burg showed in his dissertation [21] that the inverse correlation matrix could be expressed as

$$R^{-1} = ADA^\dagger \quad (24)$$

Direct solution of Eqn. (20) by matrix inversion has been documented by Barrodale and Erickson [14] and will be referred to as the Barrodale-Erickson Algorithm (BEA). Unfortunately, such inversion requires $O(m^3)$ operations, and Marple [6] has proposed an alternative algorithm which exploits the structure $[r_m(i,j)]$ and requires $O(m^2)$ operations. This algorithm will hereafter be referred to as Marple's Least-Squares Algorithm (MLSA). The BEA and MLSA techniques eliminate SLS and significantly reduce the bias and variance of the resulting spectral estimates. Additional observations regarding these two least-squares algorithms are included in Section IV.

F. AR Parameter Estimation for Long Data Records

The Maximum Likelihood Estimator (MLE) is essentially equivalent for $N \gg m$ to solving the YWE using Eqn. (13) to find estimates of $\hat{R}(k)$. Unfortunately, finding the exact MLE solution of the AR(m) parameter set is difficult. Consequently, three sequential estimation schemes for updating $\{a_m(k)\}$ of a slowly varying AR(m) process are documented by Kay & Marple [2, pp. 1393-5). They include a recursive least squares method which resembles Kalman filtering, an adaptive LPF which uses a gradient technique with corresponding slow convergence, and a lattice filter which provides updates only for the reflection coefficients coupled with the LDE to update the remaining $m-2$ coefficients. The applications contemplated in this study are restricted to short records.

G. AR Model Order Selection

The technique employed in either LSSE or MESE has been to increase the LPF order (m) until the resulting error energy (E_m) reaches some acceptable level. Unfortunately, it follows from Eqn. (11) that $E_{m+1} < E_m$ and it has been shown for an AR(M) process that the estimated spectrum is highly smoothed when $m \ll M$ and spurious detail results when $m \gg M$. Akaike has proposed two prediction estimators which have received considerable attention, the Final Prediction Error (FPE) and the Akaike Information Criterion (AIC) which for a m^{th} - order LPF are given by

$$FPE_m = \left[\frac{N+m+1}{N-m-1} \right] E_m$$

and

(22)

$$AIC_m = \ln(E_m) + 2(m+1)/N .$$

A third estimator due to Parzen [15] called the Criterion Autoregressive Transfer (CAT) is given by

$$CAT_m = \left[\frac{1}{N} \sum_{i=1}^m \hat{E}_i^{-1} \right] - \hat{E}_m^{-1}$$

where

(23)

$$\hat{E}_i = \frac{N}{N-1} E_i .$$

errors (presumed to be known). The reflection coefficients so derived are given by

$$K_{m+1} = -2 \frac{\sum_{i=m+1}^{N-1} b_m^*(i-1) f_m(i)}{\sum_{i=m+1}^{N-1} (|b_m(i-1)|^2 + |f_m(i)|^2)} \quad (17)$$

where Andersen [7] provided a flowchart for the Burg algorithm, and in a later paper [13] provided a recursive relation for the denominator (D_{m+1}) of Eqn. (17),

$$D_{m+1} = D_m \cdot (1 - |K_m|^2) - |b_m(N-m-1)|^2 - |f_m(m+1)|^2 \quad (18)$$

The computer program based on the original Andersen flowchart [7] was used by Tranter [8] and will hereafter be referred to as Andersen's Burg Algorithm (ABA). The ABA technique has several problems including spectral line splitting (SLS) and significant bias and variance in the PSD estimate.

E. Least-Squares Spectral Estimation (LSSE)

The LSSE technique removes the LDE constraint and partially differentiates Eqn. (16) with respect to all the $\{a_m(k)\}$, setting the results equal to zero, which yields

$$\frac{\partial E_m}{\partial a_m(i)} = 2 \sum_{j=0}^m a_m(j) r_m(i, j) = 0$$

where

$$r_m(i, j) = \sum_{k=0}^{N-m-1} x(k+m-j) x^*(k+m-i) + x(k+i) x^*(k+j). \quad (19)$$

In matrix form Eqn. (19) becomes

$$\begin{aligned} [r_m(i, j)]_{(m+1, m+1)} [a_m(i)]_{(m+1, 1)} \\ = [E_m \ 0 \ \dots \ 0]_{(1, m+1)} \end{aligned} \quad (20)$$

where the minimum prediction error energy is

$$E_m = \sum_{j=0}^m a_m(j) r_m(0, j). \quad (21)$$

D. Forward-Backward Linear Prediction (FBLP)

The FBLP technique was proposed by Burg [12] with forward and backward PEF errors given by

$$f_m(n) = x(n) + \sum_{i=1}^m a(i)x(n-i) \quad (14)$$

$$b_m(n) = x(n-m) + \sum_{i=1}^m a^*(i)x(n-m+i) ,$$

where $f_m(n) = \hat{x}(n) - \hat{x}(n)$, $x(n)$ given by Eqn. (2) with all $\{b(i)\} = 0$. Likewise $b_m(n)$, no relation to $b(i)$, represents a backward prediction error estimate of $x(n-m)$ based on "future" samples. Note that the summation limits in Eqn. (14) are restricted such that no samples of $x(n)$ outside the range $n=0$ to N are involved, i.e., no assumptions are made regarding the time series outside the N -sample interval; in contrast to Eqn. (13) where $R(k)$ is estimated based on the tacit assumption that $x(n) = 0$ for $n < 0$ or $n > N$. The forward-backward errors can be expressed by the recursion relations

$$\begin{aligned} f_m(n) &= f_{m-1}(n) + K_m b_{m-1}(n-1) \\ b_m(n) &= b_{m-1}(n-1) + K_m^* f_{m-1}(n) \end{aligned} \quad (15)$$

subject to the initial conditions $f_0(n) = b_0(n) = x(n)$. Implemented in a flowgraph form with error outputs from the previous section as inputs forms a so-called lattice PEF, two sections of which are shown in Figure 1 where (\bullet) implies a summing node. To obtain estimates for $\{a_M(k)\}$ Burg minimized the total error energy

$$E_M = \sum_{n=m}^{N-1} [|f_m(n)|^2 + |b_m(n)|^2] \quad (16)$$

subject to the LDE constraint for $a(i)$, thus insuring a stable AR filter. Setting the derivative of E_m , $m = 1, 2, \dots, M$, with respect to K_m equal to zero permits solving for $\{K_m\}$ as functions of the prior-order prediction

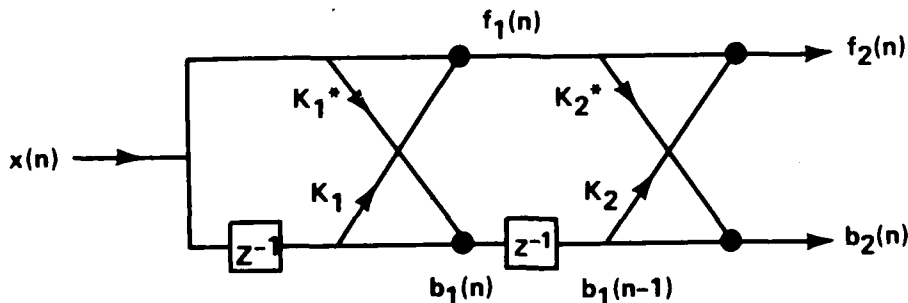


Figure 1. Lattice PEF.

$$\Delta f = \frac{1}{2\pi NT} \cos(2\phi + \theta N) \sin(\theta N) . \quad (43)$$

It is apparent that the error is a decreasing function of the number of samples used; however, when normalized with respect to the nominal DFT resolution cell width ($1/NT$), the maximum error is roughly 16% of this cell width and occurs for four values of ϕ . Swingler [46] showed that the frequency error could be reduced by inserting into the reflection coefficient expression, Eqn. (17), a Hamming weight term in both numerator and denominator summations. Moreover, independently of both Nuttall [47] and Barrodale & Erickson [14] he also proposed the least squares approach which is implemented by Marple's algorithm. A good review of noisy sinusoid spectral estimation sensitivity of the ABA to such factors as sample size, order number, phase, and SNR is detailed by Chen & Stegen [48]. It has been shown by Marple [6] that the MLSA virtually eliminates both frequency bias as a function of ϕ and SLS associated with large SNR. However, little additional has been published regarding sample size effects. The selection of order is handled routinely in MLSA by specifying MM , after which the Marple algorithm increases M until either one of the tolerance tests on error energy ratios is met or $M=MM$. The Akaike FPE first minimum test is incorporated into the BEA [14] and Tranter [8] evidently used it in deciding the order for ABA too.

Landers & Lacoss [17] noted that the various prediction error algorithms were somewhat sensitive to real vs. complex data in the presence of uniform white noise. The results for a noisy sinusoid using the ABA and MLSA are summarized for one particular test in Table 1. The value of M selected by the MLSA and corresponding frequency estimate ($F \approx f_c T = 0.05$) for 32 samples of a noisy sinusoid with $MM = 8$ are tabulated for both real and complex data. The test was repeated for the ABA using only complex data (since Δf would be a maximum at $\phi = 50^\circ$), initially with $M=8$ and then $M=3$ which was the order predicted by the first-minimum of both the FPE and CAT criteria. (The AIC had not reached a first minimum by $M=8$.) To illustrate the effect of changing N , the 10 dB SNR case was run for complex data with N reduced from 32 to 16. The spectral estimates ($M=8$) for the ABA and MLSA were 0.0500 and 0.0506, respectively. Doubling N from 32 to 64 yielded 0.0488 and 0.0497, respectively. These results would tend to show that a noisy sinusoid can be reasonably estimated for $SNR > 0$ dB even with a small number of samples. Comparative results from ABA and MLSA for real-valued noisy sinusoid ($f_c T = 0.0725$, $\alpha = 50$, $\phi = 50^\circ$) are shown in Figures A-3 and A-4. The ABA frequency bias for this particular ϕ is $NT\Delta f = 0.125$ (12.5%). It is evident from Table 1 that the initial phase is not a problem with complex-valued samples.

Table 1. MLSA and ABA Performance Comparison.

Noisy Sinusoid ($f_c T = 0.05$, $\phi = 50^\circ$, $N = 32$)

SNR	M	MLSA (MM = 8)		ABA		
		Real F	Complex M	Complex F(M=8)	Complex F(M=3)	
0.	8	0.0494	8	0.0455	0.0476	0.0440
10.	8	0.0494	8	0.0485	0.0497	0.0494
20.	8	0.4097	8	0.0497	0.0500	0.0500
30.	6	0.0500	4	0.0500	0.0500	0.0500
40.	2	0.0500	2	0.0500	0.0500	0.0500

C. Closely-Spaced-Sinusoids Estimation

The ability to resolve two closely-spaced noisy sinusoids has received considerable attention in the literature. Marple [49] empirically determined that the ability to resolve two sinusoids at frequencies f_1 and f_2 depended on the PEF order (M) and SNR (α , not in dB), i.e.,

$$\Delta F \triangleq |f_2 - f_1| T = \frac{1.023}{M[\alpha(M+1)]^{0.31}} \quad (44)$$

This formula was obtained assuming M correlation lags and is reproduced in Table 2 for M ranging from 1 to 30 and SNR ranging from 0 to 50 dB. If the number of samples $N \gg M$, Eqn. (44) serves as an upper bound on resolution, i.e, increasing M by two or three should yield equivalent resolution for a given SNR. Marple also observed that a signal of the form

$$x(k) = A_1 \cos(\theta_1 k + \phi_1) + A_2 \cos(\theta_2 k + \phi_2) \quad (45)$$

was most difficult to resolve when $\phi_1 = \phi_2$. The frequency resolution when compared to the conventional DFT periodogram was roughly four times as good as 20 dB, twice at 0 dB, and equivalent at -10 dB.

Barrodale & Erickson [14] compared their BEA with the conventional ABA and showed that it outperformed the ABA for a variety of M choices and a small number of samples. Specifically, for $N=75$ and $f_1 = 0.003$, $f_2 = 0.02$ (which corresponds to 0.23 and 1.5 cycles, respectively) the BEA program was able to identify both f_1 and f_2 correctly for $M=16$ and f_2 for $M \leq 5$, whereas the ABA generated false spectral estimates for all examples. However, they observed comparable performance if at least 15 cycles of sinusoid samples were available. Ulrych & Clayton [50] showed that their least-squares algorithm, the basis for both BEA and MLSA, had considerably less frequency bias than the ABA. They also recommended that M be selected in the range $N/3 < M < N/2$ rather than relying on the FPE or AIC first-minimum concept. This recommen-

Table 2. Frequency Resolution Estimates Using Equation 44.

M	SNR (DB)					
	0.	10.	20.	30.	40.	50.
1	0.83075	0.40689	0.19928	0.09761	0.04780	0.02341
2	0.36631	0.17941	0.08787	0.04304	0.02108	0.01032
3	0.22337	0.10940	0.05358	0.02624	0.01285	0.00630
4	0.15633	0.07657	0.03760	0.01837	0.00900	0.00441
5	0.11819	0.05789	0.02835	0.01389	0.00680	0.00333
6	0.09300	0.04599	0.02252	0.01103	0.00540	0.00265
7	0.07722	0.03782	0.01852	0.00907	0.00444	0.00218
8	0.06515	0.03191	0.01563	0.00765	0.00375	0.00184
9	0.05606	0.02745	0.01344	0.00658	0.00323	0.00158
10	0.04897	0.02399	0.01175	0.00575	0.00282	0.00138
11	0.04334	0.02123	0.01040	0.00509	0.00249	0.00122
12	0.03876	0.01898	0.00930	0.00455	0.00223	0.00109
13	0.03496	0.01712	0.00839	0.00411	0.00201	0.00099
14	0.03177	0.01556	0.00762	0.00373	0.00183	0.00090
15	0.02907	0.01424	0.00697	0.00342	0.00167	0.00082
16	0.02674	0.01310	0.00642	0.00314	0.00154	0.00075
17	0.02473	0.01211	0.00593	0.00291	0.00142	0.00070
18	0.02297	0.01125	0.00551	0.00270	0.00132	0.00065
19	0.02142	0.01049	0.00514	0.00252	0.00123	0.00060
20	0.02004	0.00981	0.00481	0.00235	0.00115	0.00056
21	0.01881	0.00921	0.00451	0.00221	0.00108	0.00053
22	0.01771	0.00867	0.00425	0.00208	0.00102	0.00050
23	0.01672	0.00819	0.00401	0.00196	0.00096	0.00047
24	0.01582	0.00776	0.00380	0.00186	0.00091	0.00045
25	0.01500	0.00735	0.00360	0.00176	0.00086	0.00042
26	0.01426	0.00698	0.00342	0.00168	0.00082	0.00040
27	0.01358	0.00665	0.00326	0.00160	0.00078	0.00038
28	0.01296	0.00634	0.00311	0.00152	0.00075	0.00036
29	0.01237	0.00606	0.00297	0.00145	0.00071	0.00035
30	0.01184	0.00580	0.00284	0.00139	0.00068	0.00033

dation is also supported by Kay & Marple [2, p. 1397] who illustrated that increasing M from four to 32 resolved two sinusoids at 0.143 and 0.200 at a SNR = 0 dB. An example [16] of spectral estimation for two equal amplitude, complex-valued sinusoids ($f_1 = 0.11$, $f_2 = 0.14$, $N=40$, $\alpha=50$) using the ABA program with $M=15$ is given in Figure 5. Spectral estimates for the two peaks differ slightly, e.g., ABA: (0.1120, 0.1388) and MLSA: (0.1105, 0.1395). The PEF-order estimators for the ABA program are shown in Table 3. Local minima for the FPE and CAT estimators track each other rather consistently, whereas the AIC estimate does not provide a local minimum through $M=15$, which is consistent with the MLSA setting $M = MM = 15$.

Table 3. PEF Order Estimators Using ABA Program ($M=15$).

Two Noisy Sinusoids ($f_{1T} = 0.11$, $f_{2T} = 0.14$, SNR = 17 dB)

	POWER - P(J)	AKAIKE - FPE(J)	AKAIKE - AIC(J)	PARZEN - CAT (J)
J= 1	0.9634051E-01	0.1061502E+00	-0.6371941E+02	-0.0288167E+01
J= 2	0.8574154E-01	0.1029001E+00	-0.5697115E+02	-0.1200734E+02
J= 3	0.8649273E-01	0.1057013E+00	-0.6791240E+02	-0.0700143E+01
J= 4	0.7319263E-01	0.9410481E-01	-0.7495642E+02	-0.1119740E+02
J= 5	0.6463443E-01	0.8744659E-01	-0.796F032E+02	-0.1012044E+02
J= 6	0.5770326E-01	0.8218314E-01	-0.8409781E+02	-0.1022709E+02
J= 7	0.5085630E-01	0.7628445E-01	-0.8915027E+02	-0.1421729E+02
J= 8	0.4834229E-01	0.7641162E-01	-0.9117817E+02	-0.1397511E+02
J= 9	0.4815539E-01	0.8225692E-01	-0.9133259E+02	-0.1326657E+02
J= 10	0.4414519E-01	0.7763464E-01	-0.9481022E+02	-0.1353770E+02
J= 11	0.4247440E-01	0.7882102E-01	-0.9635415E+02	-0.1319240E+02
J= 12	0.3724384E-01	0.7318828E-01	-0.1016107E+03	-0.1444856E+02
J= 13	0.3539201E-01	0.7350648E-01	-0.1036508E+03	-0.1424200E+02
J= 14	0.3332665E-01	0.7331863E-01	-0.1060559E+03	-0.1410201E+02
J= 15	0.3102525E-01	0.7239226E-01	-0.1082162E+03	-0.1433036E+02

Tranter [8] developed a real-valued ($N=100$) test case for Eqn. (45) in which the chosen frequencies ($f_1 = 0.098$, $f_2 = 0.102$) were spaced less than one-half a DFT cell apart. Both he and Shumway [10] used the BEA program in conjunction with the FPE first-minimum criterion to study the effects of SNR on the spectral estimation and concluded that proper resolution required at least 40 dB SNR. This value turns out to be too large because of their reliance on the FPE first-minimum criterion to select M.

The results obtained by repeating this test case using MLSA on real data for a variety of SNR-M combinations are summarized in Table 4 and some responses are shown in Figure 6. It is apparent that the test frequencies can be resolved with less than 1% error for a SNR of 20 dB provided M is large enough. In contrast, an M of 7 can be used when the SNR = 50 dB. The third column of Table 4 labeled $S(0.1)$ indicates the response in dB at the mid-point ($F=0.1$) relative to the smaller sinusoid, with 0 dB indicating failure to resolve the two components. The final column (M_e) indicates the value of M predicted from Table 2 which should yield a response similar to the 33/20 dB curve in Figure 6 for that particular SNR. As stated earlier M_e is based upon autocorrelation estimates rather than data samples; however, the difference between it and the M which yields $S(0.1) = 3$ dB is evidently a function of SNR, ranging from approximately nine at 20 dB to three at 50 dB.

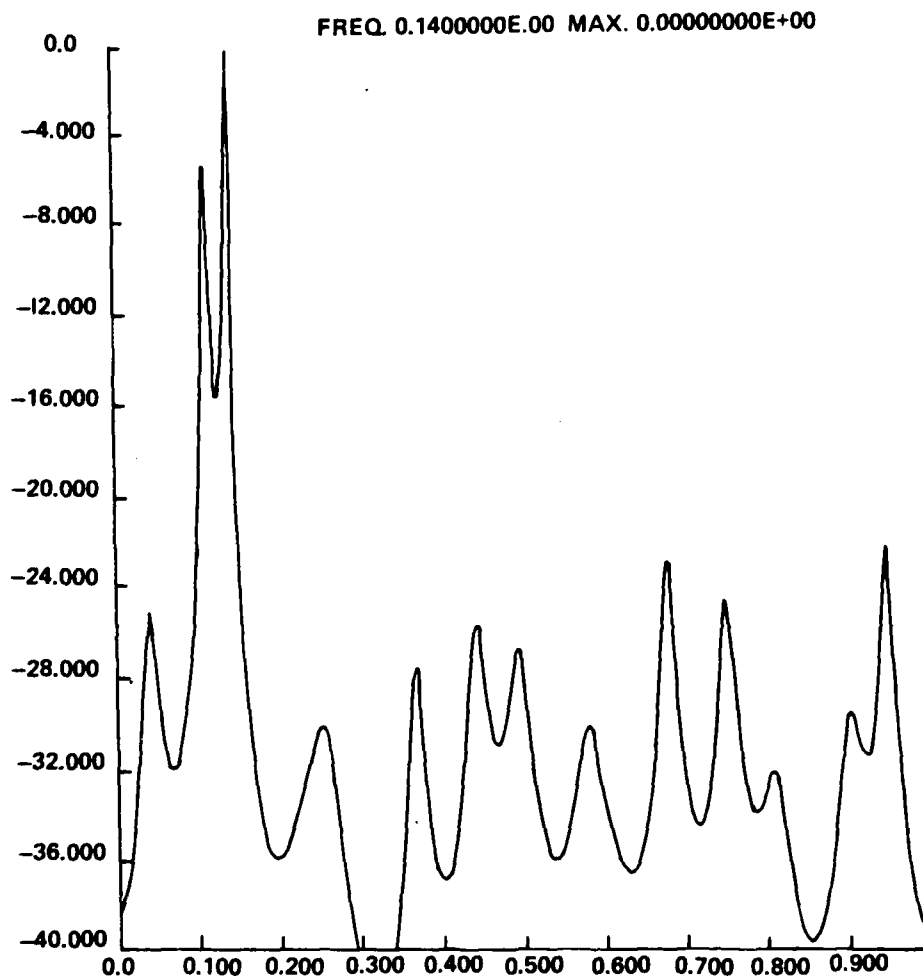


Figure 5. Double sinusoid spectral estimate using ABA.

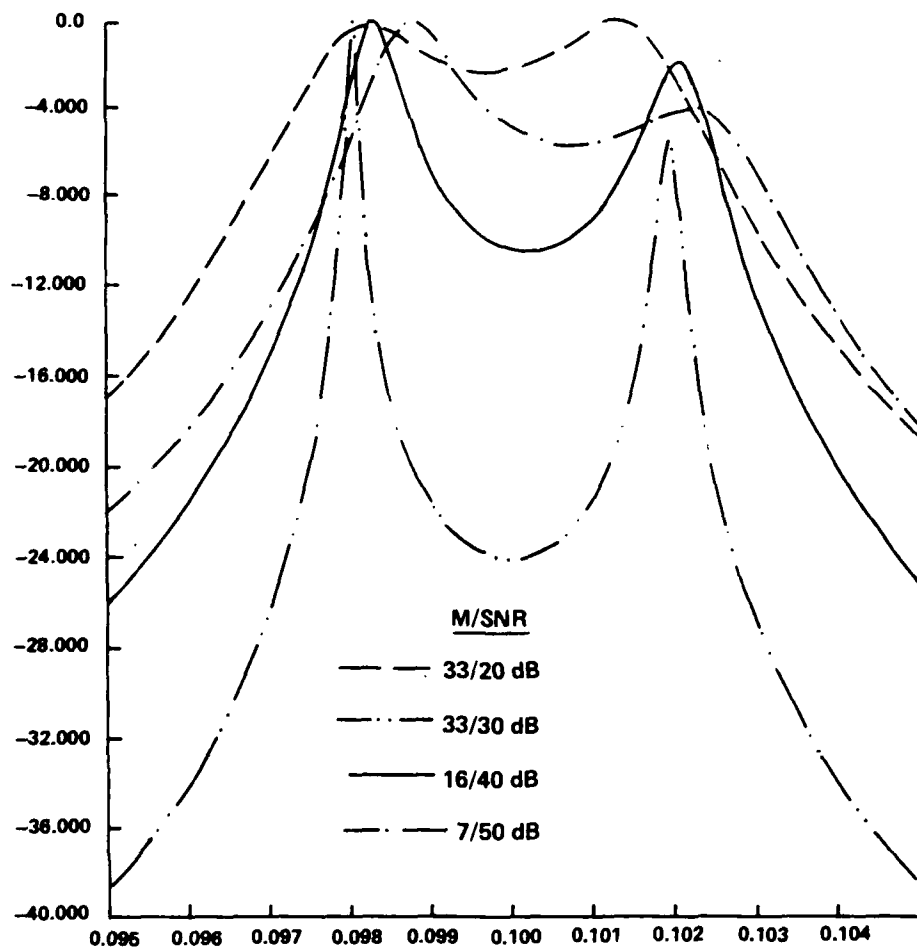


Figure 6. Tranter's test case using MLSA.

Table 4. Summary of Tranter's Test Case Using MLSA.

M	SNR (dB)	S(0.1) dB	M _e
33	20	2.5	24
33	30	24.0	14
16	30	0.	14
16	40	10.5	8
10	50	18.5	5
7	50	2.0	5
5	50	0.	5

D. Target Identification

Target identification is a potential radar application for the ability of MSA techniques to resolve closely-spaced sinusoids. Unfortunately, little has been found in the open literature regarding this feature and time did not permit a search of the classified literature. Taylor *et. al.* [51] described one situation in which the DFT and MEM techniques were both applied to two sweep-scan radar-return data sets (N=64) from a single-engine jet aircraft. Basically, the MEM spectrum was able to identify spectral lines in both data sets for the target doppler and upper modulation sideband (caused by engine turbine rotation), whereas the DFT spectrum was poorer and failed to identify the modulation sideband for one data set. A classified report by Gardner [52] indicates that more complicated spectral returns would be needed to distinguish various types of aircraft. Only Swingler [45] seems to have addressed the resolution of more than two sinusoids, providing some information regarding the resolvability of ten harmonically related sinusoids with relative amplitudes in the range 0.1 to 1.0 with 5% added white noise. Time did not permit simulation of this situation nor the review of some specialized techniques to resolve sinusoids in the presence of noise. These methods, reviewed by Kay & Marple [2, pp. 1402-7] include Pisarenko Harmonic Decomposition, Prony Spectral Line Decomposition and Prony's Method (Extended) with appropriate references cited. In each case the number of sinusoids must be estimated to establish a model order. Other recent papers on this topic have been written by Tufts & Kumaresan [53, 54] Kay [55], Marple [56, 57], and Shumway [10].

V. RESULTS AND RECOMMENDATIONS

The basic theory of MSA was traced from the Yule-Walker equations, which assumed the autocorrelation function was either known or could be approximated, thru the forward-backward energy minimization of Burg, to the algorithms of Andersen, Barrodale & Ericksen, and Marple which are used in MSA. The various model-order selection schemes were used with both AR and noisy-sinusoid signals. Sawyer's method was recorded for determining the inverse of the correlation matrix using iterative equations which are functions of the M^{th} order LPF coefficients.

Clutter modeling and subsequent suppression by inverse filtering seems to be a definite application of MSA. It was shown that clutter is basically modeled spectrally as an AR process and the McMaster University team (Haykin, et. al.) demonstrated that both simulated and real clutter PSD could be modeled adequately by MSA, particularly when the samples were complex valued. Using theory developed in the late 1960s, Sawyers demonstrated the feasibility of designing a DFB, which would optimally improve the SIR, by multiplying the inverse-R matrix by a steering vector. This matrix could be obtained by traditional means, if the clutter correlation function was specified, or by the use of MSA as discussed earlier when only clutter-dominated sample returns were available. Adaptive filtering based on this technique has been studied also by Nitzberg in support of a U. S. Air Force RADC project. Gibson & Haykin have studied properties of adaptive lattice PEF required to suppress clutter. Such filters require computation only of reflection coefficients obtained from Burg's forward and backward errors. Decoupling appears to be a problem since all coefficients initially adapt to the strongest spectral component and once K_1 is fixed, the remaining values readjust to the next strongest component, etc. Their research indicated roughly three stages for every broad peak in the PSD and one for each sharp peak.

Resolution of two sinusoids was studied for a variety of SNR values. It was shown that the conventional model-order predictors of Akaike and Parzen tended to produce a first-minimum at too low an order. Marple's technique seems to be more appropriate; however, the tolerance choices must be selected with some care. Marple's empirical formula for frequency resolution capability as a function of model order and SNR, as reproduced in Table 2, seems to provide a reasonable starting point for selecting M for a particular SNR. Studies performed in Section IV tend to indicate that true AR(M) processes can be spectrally estimated quite well with $m \approx M$ and noisy sinusoid pairs can be resolved with large m, typically approaching $N/3$ for low SNR.

It is recommended that clutter suppression algorithm be designed with Quiet Radar parameter sets and tested with complex data obtained from the radar. It is also suggested that the MLSA be applied to the problem of multiple sinusoid estimation where the amplitude-frequency assignment is chosen to emulate the spectrum associated with a particular type or class of targets. Finally, contacts should be initiated with researchers at McMaster University, RADC, and in other organizations where work is underway on the clutter suppression problem.

REFERENCES

1. R. Houts, "Applications of spectral estimation techniques to radar data, Battelle Report (D.O. 1876) to U. S. Army Missile R & D Cmd., Sept. 1981.
2. S. Kay and S. Marple Jr., "Spectrum analysis - a modern perspective," Proc. IEEE, vol. 69, Nov. 1981, pp. 1380-1419.
3. L. Brennan and L. Reed, "Theory of adaptive radar," IEEE Trans. AES, vol. AES-9, Mar. 1973, pp. 237-52.
4. A. Rihaczek, "The maximum entropy of radar resolution," IEEE T. AES, vol. AES-17, Jan. 1981, p. 144.
5. P. Jackson, "Radar superresolution? Perhaps!" IEEE T. AES, vol. AES-17, Sep. 1981, pp. 734-5.
6. _____, "A new autoregressive spectrum analysis algorithm," IEEE Trans. Acoust., Speech, Signal Process., vol. ASSP-28, pp. 441-454, Aug. 1980.
7. N. O. Andersen, "On the calculation of filter coefficients for maximum entropy spectral analysis," Geophys., vol. 39, pp. 69-72, Feb. 1974.
8. W. Tranter, "A comparison of autoregressive spectral analysis techniques," Battelle Report (D.O. 1044) to U.S. Army Missile R & D Cmd., Oct. 1979.
9. ----, "Noise compensation applied to a maximum entropy spectral analysis routine," Battelle Report (D.O. 1803) to U. S. Army Missile R & D Cmd., Jan. 1982.
10. R. Shumway, "On maximum entropy and periodic regression as methods for resolving contiguous-frequency power spectra, Battelle Report (D.O. 1894) to U.S. Army Missile R & D Cmd., De. 1981.
11. J. P. Burg, "Maximum entropy spectral analysis." in Proc. 37th Meeting Society of Exploration Geophysicists (Oklahoma City, OK), Oct. 31, 1967.
12. .[38]_____, "A new analysis technique for time series data," NATO Advanced Study Institute on Signal Processing with Emphasis on Underwater Acoustics, Enschede. The Netherlands, Aug. 12-23, 1968.
13. _____, "Comments on the performance of maximum entropy algorithms," Proc. IEEE, vol. 66, pp. 1581-1582, Nov. 1978.
14. I. Barrodale and R. E. Erickson, "Algorithms for least-squares linear prediction and maximum entropy spectral analysis-Part I: Theory and Part II: FORTRAN Program," Geophys., vol. 45, pp. 420-446, Mar. 1980.

15. _____, "Some recent advances in time series modeling," IEEE Trans. Automat. Contr., vol. AC-19, pp. 723-730, Dec. 1974.
16. T. J. Ulrych and T. N. Bishop, "Maximum entropy spectral analysis and autoregressive decomposition." Rev. Geophysics Space Phys., vol 13, pp. 183-200, Feb. 1975.
17. T. W. Anderson, "Estimation by maximum likelihood in autoregressive moving average models in the time and frequency domains," Dep. Statistics, Tech. Rep. 20, Contract NR-042-034, Stanford University, Stanford, CA, June 1975
18. T. E. Landers and R. T. Lacoss, "Some geophysical applications of autoregressive spectral estimates." IEEE Trans. Geosci. Electron., vol. GE-15, pp. 26-32, Jan. 1977.
19. S. M. Kay, "The effects of noise on the autoregressive spectral estimator," IEEE Trans. Acoust., Speech, Signal Process., vol. ASSP-27, pp. 478-485, Oct. 1979.
20. _____, "Noise compensation for autoregressive spectral estimates," IEEE Trans. Acoust., Speech, Signal Process., vol. ASSP-28, pp. 292-303, June 1980
21. _____, "Maximum entropy spectral analysis," Ph. D. dissertation, Dep. Geophysics, Stanford Univ., Stanford, CA, May 1975
22. R. Herring, "Maximum entropy spectral analysis and radar signal processing," Technical Report TR-2 of Technical Panel KTP-3 (Radar Signal Processing), Nov. 1979.
23. R. Nitzberg, "Some design details of the application of modern spectral estimation techniques to adaptive processing," Proc. First ASSP Workshop on Spectral Estimation, Aug. 1981, paper 7.1.
24. M. Siddiqui, "On the inversion of the sample covariance matrix in a stationary autoregressive process," Annals of Math. Statistics, vol. 29, 1958, pp. 585-8.
25. J. Sawyers, "Adaptive pulse-doppler radar signal processing using the maximum entropy method," IEEE 1980 EASCON Record, pp. 454-61.
26. S. Zahner and N. Currie, "Radar clutter modeling for the quiet radar," Battelle Report (D.O. 1544) to U.S. Army Missile R & D Cmd., Dec. 1980, pp. 12 and 38.
27. M. Abramowitz and I Stegun (Eds.), Handbook of Mathematical Functions, Nat. Bureau of Stds., Washington D.C., p. 932.
28. ----, "Modeling of clutter for coherent pulsed radar," IEEE T. Info. Theory Nov. 1975, pp. 703-7.
29. S. B. Kesler and S. S. Haykin, "The maximum entropy method applied to the spectral analysis of radar clutter," IEEE Trans. Inform. Theory, vol. IT-24, pp. 269-272, Mar. 1978.

30. S. Kesler and S. Haykin, "A comparison of the maximum entropy and the periodogram method applied to the spectral analysis of computer-simulated radar clutter," Canadian Electrical Eng. Jour., Vol. 3, Jan. 1978, pp. 11-16.
31. _____, "Maximum entropy estimation of radar clutter spectra," in Natl. Telecommunications Conf. Rec. (Birmingham, AL), pp. 18.5.1-18.5.5, Dec. 3-6, 1978.
32. S. Haykin, S. Kesler, and B. Currie, "An experimental classification of radar clutter," Proc. IEEE, vol. 67, Feb. 1979, pp. 332-3.
33. C. Hawkes and S. Haykin, "Adaptive digital filtering for coherent MTI radar," Record IEEE 1975 Int. Radar Conf., pp. 57-62.
34. W. Rummier, "Clutter suppression by complex weighting of coherent pulse trains," IEEE Trans. AES, vol. AES-2, Nov. 1966, pp. 689-99.
35. L. Spafford, "Optimum radar signal processing in clutter," IEEE Trans. IT, vol. IT-14, Sept. 1968, pp. 734-43.
36. J. Hunter, R. Hyneman, and J. Sawyers, "Design and implementation of Hughes AN/TPQ-37 artillery locating radar signal processor," Tri-Services Radar symposium, Jul. 1976, pp. 222-4.
37. D. E. Bowyer, P. K. Rajasekaran, and W. W. Gebhart. "Adaptive clutter filtering using autoregressive spectral estimation." IEEE Trans. Aerospace Elec. Syst., vol. AES-15. pp. 538-546. July 1979
38. J. H. Sawyers, "Applying the maximum entropy method to adaptive digital filtering," in Rec. 12th Asilomar Conf. Circuits, Systems and Computers, pp. 198-202.
39. J. Gibson, S. Haykin, and S. B. Kesler, "Maximum entropy (adaptive digital filtering applied to radar clutter." in Rec. 1979 IEEE Int. Conf. Acoustics, Speech, and Signal Processing, pp. 166-169.
40. _____, "Stable and efficient lattice methods for linear prediction." IEEE Trans. Acoust., Speech, Signal Processing, vol. ASSP-25, pp. 423-428, Oct. 1977.
41. C. Gibson and S. Haykin, "A comparison of algorithms for the calculation of adaptive lattice filters," Proc. 1980 IEEE Int. Conf. ASSP, pp. 978-83.
42. L. Griffith, "A continuously-adaptive filter implemented as a lattice structure," Proc. 1977 IEEE Conf. ASSP, pp. 683-6.
43. ----, "Learning characteristics of adaptive lattice filtering algorithms," IEEE Trans. ASSP, vol. ASSP-28, Dec. 1980, pp. 681-91.

44. ----, "Performance studies of adaptive lattice prediction-error filters for target detection in a radar environment using real data, "Proc. 1981 IEEE Conf. ASSP, pp. 1054-7.
45. D. N. Swingler, "A comparison between Burg's maximum entropy method and a nonrecursive technique for the spectral analysis of deterministic signals," *J. Geophysical Res.*, vol. 84, pp. 679-685, Feb. 10, 1979.
46. _____, "A modified Burg algorithm for maximum entropy spectral analysis," *Proc. IEEE*, vol. 67, pp. 1368-1369, Sept. 1979.
47. _____, "Spectral analysis of a univariate process with bad data points, via maximum entropy, and linear predictive techniques." Naval Underwater Systems Center, Tech. Rep. 5303, New London, CT. Mar. 26, 1976.
48. W. Y. Chen and G. R. Stegen, "Experiments with maximum entropy power spectra of sinusoids," *J. Geophysical Res.*, vol. 79, pp. 3019-3022, July 10, 1974.
49. _____, "Frequency resolution of high-resolution spectrum analysis techniques," in *Proc. 1978 RADC Spectrum Estimation Workshop*, pp. 19-35.
50. T. J. Ulrych and R. W. Clayton, "Times series modelling and maximum entropy," *Phys. Earth Planetary Interiors*, vol. 12, pp. 188-200, Aug. 1976.
51. R. Taylor, T. Durrani, and C. Goutis, "Block processing in pulse doppler radar," IEE Int. Conf. Radar-77, Oct. 1977, pp. 373-8.
52. R. Gardner, "Aircraft radar target signatures (U), "Naval Research Laboratory Report 7156 (Secret), Sept. 15, 1970.
53. R. Kumaresan and D. W. Tufts, "Improved spectral resolution III: Efficient realization," *Proc. IEEE*, vol. 68, pp. 1354-1355, Oct. 1980.
54. D. W. Tufts and R. Kumaresan, "Improved spectral resolution," *Proc. IEEE*, vol. 68, pp. 419-420, Mar. 1980.
55. S. Kay, "More accurate autoregressive parameter and spectral estimates for short data records, "Proc. First ASSP Workshop on Spectral Estimation, Aug. 1981, paper 2.1.
56. S. Marple Jr., "Spectral Line Analysis - Batch and Sequential Adaptive Approaches, "IEEE First ASSP Workshop on Spectral Estimation, Aug. 1981, paper 4.4.
57. ----, "Exponential Energy Spectral Density Estimation, "Proc. 1980 IEEE Conf. ASSP, pp. 588-91.

58. S. Haykin and S. Kesler, "The complex form of the maximum entropy method for spectral estimation." Proc. IEEE, vol. 64, pp. 822-823, May 1976.
59. A. K. Datta. Comments on "The complex form of the maximum entropy method for spectral estimation." Proc. IEEE, vol. 65, pp. 1219-1220, Aug. 1977.
60. S. B. Bowling, "Linear prediction and maximum entropy spectral analysis for radar applications." M.I.T. Lincoln Lab., Project Rep. RMP-122 (ESD-TR-77-113), May 24, 1977.

ACRONYM LIST

ABA	Andersen's Burg Algorithm
AIC	Akaike Information Criterion
AR	Autoregressive
AR(m)	AR process of m^{th} -order
ARMA	Autoregressive Moving Average
BEA	Barrodale-Erickson Algorithm
CNR	Clutter-to-Noise Ratio
DFB	Doppler Filter Bank
DFT	Discrete Fourier Transform
FBLP	Forward-Backward Linear Prediction
FPE	Final Prediction Error
LDE	Levinson-Durbin Equation
LPF	Linear Prediction Filter
LSSE	Least-Squares Spectral Estimation
MEM	Maximum Entropy Method
MESE	Maximum Entropy Spectral Estimation
MLE	Maximum Likelihood Estimator
MLSA	Marple's Least-Squares Algorithm
MSA	Modern Spectral Analysis
MTI	Moving Target Indicator
PDF	Probability Density Function
PEF	Prediction Error Filter
PHD	Pisarenko Harmonic Decomposition
PSD	Power Spectral Density
SCR	Signal-to-Clutter Ratio

ACRONYM LIST (Cont'd)

SIR	Signal-to-Interference Ratio
SLS	Spectral Line Splitting
SNR	Signal-to-Noise Ratio
YWE	Yule-Walker Equations

APPENDIX

MSA PROGRAM

The computer program listed in Figure A-1 of this appendix is basically an extension to complex data of Tranter's program [8]. The complex-data extension is based on the algorithm of Haykin & Kesler [58], Datta [59] and Bowling [60]. The BEA [14] used by Tranter for LSSE was replaced by Marple's algorithm [6] because it is computationally more efficient and has its own prediction-order estimator, which was shown in Section IV to be better than the conventional estimators of Akaike and Parzen used herein in conjunction with the ABA option. Marple estimates that his LSSE algorithm requires only 20% more computation time than the ABA program, whereas Tranter estimated that the BEA program took three times as long. An X-Y plot routine written by Tom Cash for the PDP 11/34 computer was also included in the MSA program.

The main program is designed to read user control parameters (see Table A-1), generate the real (imaginary) noise power σ^2 consistent with the user supplied SNR and Eqn. (42), call the appropriate subroutines (S.R.), remove any bias (mean value) from the generated samples, write appropriate output information information, and generate PSD (dB) vs. frequency (Hz) data points for S.R. PLT. The various subroutines and their purposes are itemized in Table A-1 in the order in which they are listed in Figure A-1.

Some examples of the printouts and PSD plots achieved with the ABA and MLSA follow. The common header describing the test case data is deleted from the b-part of Figures A-2 and A-3 to insure a one-page fit.

Table A-1. Input Parameters for Program MSA.

<u>Card</u>	<u>Symbols</u>	<u>Function</u>
1	ISIG	Test flag indicating presence (=1) or absence (=0) of sinusoids, Eqn. (45).
	ICLT	<u>Ibid.</u> for AR(MC), Eqn. (2).
	ICPX	Data samples are real (=0) or complex (=1).
	IALG	Estimation technique is ABA (=0) or MLSA (=1).
2	SNRDB	SNR (dB) (ISIG=1).
	CNRDB	CNR (dB) (ICLT=1).
3	A1, F1, PHI1	Amplitude, frequency, and initial phase of first sinusoid in Eqn. (45). (ISIG=1).
4	A2, F2, PHI2	<u>Ibid.</u> for second sinusoid.
5	N	Number of samples in test waveform.

```

COMPLEX AREAN,X(250),AL250),Y(250)
DIMENSION PSDDB(250),FREQ(250),PSD(250),PE(50)
DIMENSION FPE(50),P(50),AR(5),AIC(50),CAT(50)
REAL NPR,NSU
SIGPR=0.
CPOU=0.
SIGNA=1.
CALL ASSIGN(3,'DK1:CRS.NE',10,'OLD')
READ(3,100) TSG,ICLT,ICPX,IALG
READ(3,101) SHRDB,CHRDB
READ(3,101) A1,F1,PH11
READ(3,101) A2,F2,PH12
READ(3,100) M,N,NC,K
READ(3,101) FN,FL,FF,TOLL,TOL2
READ(3,101) AR
FORMAT(1013)
FORMAT(5C16.8)
WRITE(7,150)
FORMAT(//,' SIMULATION VARIABLES'//)
C
SINUSOID DATA
WRITE(7,250) A1,F1,PH11,A2,F2,PH12
FORMAT(15X,'A1',E12.5,10X,'F1',E12.5,
1 10X,'PH11',E12.5,5X,'A2',E12.5,10X,
2 'F2',E12.5,10X,'PH12',E12.5/)
PH11=0.01745338PH11
PH12=0.01745338PH12
SIGPR=(A1122+A2122)
IF(ICPX.EQ.0) SIGPR=SIGPR/2.
SHR=10.081(SHRDB/10.0)
SIGMA=SQRT(SIGPR*(SHR+2.))
IF(ICPA.EQ.0) SIGMA=SIGMA*SQRT(2.)
CALL SIG1(N,FR,A1,F1,PH11,A2,F2,PH12,X)
AR CLUTTER DATA
CONTINUE
IF(ICLT.EQ.0) GO TO 2
CALL ARECLTR(N,NC,AR,X)
CALL NPLB(X,N,CPOU)
CNR=10.21(CNRDB/10.)
SIGMA=SQRT(CPOU/CNR)
WRITE(7,303) AR
FORMAT(15X,'AR CLUTTER COEFF.',5E15.5)
C
303
C
CALL GASS(SIGMA,V,N)
CALL NPLBY(N,NPR)
IF(ICPA.EQ.0) NPR=NPR/2.
AREAN=0.
FLTH=FLOAT(R)
DO 112 J=1,N
X(J)=X(J)+Y(J)
IF(ICPA.EQ.0) X(J)=REAL(X(J))
AREAN=AREAN+X(J)
112 CONTINUE
AREAN=AREAN/CPLX(FLTH,0.)
DO 113 J=1,N
X(J)=X(J)-AREAN
CALL NPLBY(N,NSU)
WRITE(7,301) SHRDB,SIGPR,NPR,CHRDB,CPOU,NSU
FORMAT(15X,'SHRDB',F10.0,9X,'SIGPR',
3 F10.0,9X,'NPR',F10.5/5X,'CHRDB',F10.0,9X,
1 F10.0,9X,'NSU',F10.5)
301
302
FORMAT(15X,'No.',14,10X,'No.',14,10X,'NC',14/)

```

```

C
IF(IALG.EQ.0) GO TO 3
SAMPLE ALGORITHM
IF(TOLL.EQ.0.) TOLL=0.001
IF(TOL2.EQ.0.) TOL2=0.005
MVAR=N
CALL MAPLE(N,R,PMAX,X,A,E,TOLL,TOL2,ISTA,EO,PE)
WRITE(7,300) MLE,E
FORMAT(//,' SAMPLE ALGORITHM R=',12,5X,'E(0)',E12.4,5X,
1 E(1),E12.4//,' SEARCH TERMINATION STATUS'//)
IF(ISTA.EQ.1) WRITE(7,361)
IF(ISTA.EQ.2) WRITE(7,362)
IF(ISTA.EQ.3) WRITE(7,363)
IF(ISTA.EQ.4) WRITE(7,364) TOLL
IF(ISTA.EQ.5) WRITE(7,365) TOL2
FORMAT(15X,'R',PMAX//)
FORMAT(15X,'DEN(M)',LE,0-ERROR//)
FORMAT(15X,'E(M)',GT,1-ERROR//)
FORMAT(15X,'E(M)/E(0)',LT,TOLL,E10.4)
FORMAT(15X,'(E(M)-E(R))/(E(R)-1)',LT,TOL2,E10.4)
GO TO 4
C
BURC ALGORITHM
CALL MRC(N,M,R,A,P)
CALL FPE1(N,M,P,FPE,AIC,CAT)
C
4
COMPUTE POWER SPECTRUM
CALL MPEGR(FR,A,FI,FF,AR,K,PSD,PEAK)
IF(IALG.EQ.0) GO TO 6
WRITE(7,600) (J,A1J),PE(J),J=1,N)
FORMAT(//,15X,'AR COEFFICIENTS',25X,'PRED. ERROR ENERGY',
1 '-',E(J)//(10X,'A',12.),'E15.7,E15.7,15X,E12.4)
GO TO 750
600
700
FORMAT(//17X,'PRED. ERROR COEFF. - A(J)',
1 10X,'POWER - P(J)',7X,'AKAIKE -',
2 'FPE(J)',3X,'AKAIKE - AIC(J)',4X,
3 'PMARZEN - CAT(J)',//)
DO 750 J=1,N
WRITE(7,710) J,A1J),P(J),FPE(J),AIC(J),CAT(J)
710
FORMAT(15X,'J',13,5X,E15.7,E15.7,415X,E15.7))
750 CONTINUE
800
WRITE(7,800) PEAK
FORMAT(//10X,'PEAK SPECTRAL FREQ.',F8.3,' MZ',/
DO 950 J=1,K
FREQ(J)=FI+DRG*FLOAT(J-1)
PSDDB(J)=10.0*ALOC10(PSD(J))
950 CONTINUE
PAUSE
CALL PLT(FREQ,PSDDB,K)
CONTINUE
STOP
END
C
SUBROUTINE SIG1(N,FR,A1,F1,PH11,A2,F2,PH12,X)
C THIS ROUTINE GENERATES THE SIGNAL SAMPLES
C
C
C N NUMBER OF POINTS
C FN SAMPLING FREQUENCY
C A1,A2 COMPONENT AMPLITUDES
C F1,F2 COMPONENT FREQUENCIES
C PH11,PH12 COMPONENT PHASES
C X OUTPUT ARRAY

```

Figure A-1. Computer program for MSA.

```

COMPLEX X(I)
TPI=6.283185308
DO 100 J=1,N
F(J)=TPI*FLOAT(J-1)/FM
CA=ARCOS(F1*F(J)*PHI1)
BA=ASIN(F1*F(J)*PHI1)
CB=ARCOS(F2*F(J)*PHI2)
SB=ASIN(F2*F(J)*PHI2)
XB=CA+CB
XI=SA+SB
X(I)=CMPLX(XB,XI)
100 CONTINUE
RETURN
END

SUBROUTINE GASS(SIGMA,Y,N)
GENERATES GAUSSIAN PROCESS
SIGMA STANDARD DEVIATION
Y OUTPUT ARRAY
N NUMBER OF POINTS
COMPLEX Y(I)
K1=22307
K2=11353
PI2=6.283185308
DO 55 J=1,N
U1=RN(K1,K2)
UB=RN(K1,K2)
GAS=SQRT(-2)*ALOG(U1)/COS(PI2*U2)
Y(J)=SIGMA*CMPLX(GAS,GAI)
55 CONTINUE
RETURN
END

SUBROUTINE INPRT(Y,N,APR)
READS REAL-SQUARE VALUE
Y INPUT ARRAY
N NUMBER OF POINTS
APR NOISE POWER
COMPLEX Y(I)
SUM=0
DO 100 J=1,N
SUM=SUM+Y(J)*CONJUG(Y(J))
100 CONTINUE
APR=SUM/FLOAT(N)
RETURN
END

SUBROUTINE FPE(IN,R,P,FPE,AIC,CAT)
COMPUTES PREDICTION ERROR ESTIMATES
IN NUMBER OF POINTS
R ORDER OF FILTER
P ARRAY OF PREDICTION ERRORS
COMPLEX X(I)
TPI=6.283185308
DO 100 J=1,N
F(J)=TPI*FLOAT(J-1)/FM
CA=ARCOS(F1*F(J)*PHI1)
BA=ASIN(F1*F(J)*PHI1)
CB=ARCOS(F2*F(J)*PHI2)
SB=ASIN(F2*F(J)*PHI2)
XB=CA+CB
XI=SA+SB
X(I)=CMPLX(XB,XI)
100 CONTINUE
APR=SUM/FLOAT(N)
RETURN
END

SUBROUTINE FREG(FM,A,FI,FF,M,K,PSD,PEAK)
CALCULATES FREQUENCY RESPONSE
FM SAMPLING FREQUENCY
A ARRAY OF FILTER COEFFICIENTS
FI INITIAL FREQUENCY TO BE OUTPUT
FF FINAL FREQUENCY TO BE OUTPUT
M ORDER OF FILTER
K NUMBER OF POINTS TO BE OUTPUT
PSD ARRAY OF POWER SPECTRAL DENSITY POINTS
PEAK FREQUENCY OF SPECTRAL PEAK
COMPLEX A(I)
DIMENSION PSD(I)
COMPLEX SUM,C
TPI=6.2831853
DF=(FF-FI)/FLOAT(K-1)
DO 100 J=1,K
SUM=CMPLX(1.0,0.0)
D=-TPI*(FI+DF*FLOAT(J-1))/FM
DO 200 M=1,M
B=DF*FLOAT(M)
C=CMPLX(0.0,B)
SUM=SUM+(A(M)*EXP(C))
200 CONTINUE
PSD(J)=1.0/(CABS(SUM)*CABS(SUM))
100 CONTINUE
APR=0.0
DO 150 J=1,K
APR=MAXI(APR,PSD(J))
IF(PSD(J).EQ.APR) MF=J
150 CONTINUE
DO 160 J=1,K
PSD(J)=PSD(J)/APR
160 CONTINUE
PEAK=FLOAT(MF-1)*DF+FI
RETURN
END

SUBROUTINE PLT(X,Y,NPTS)
LINE WITH TITLE
DIMENSION Y(SI2),X(SI2)
CALL BEGIN

```

Figure A-1. Computer program for MSA. (Cont'd)


```

C      ORDER N
C      TOL1 = TOLERANCE FACTOR THAT STOPS RECURSION AT ORDER N
C      WHEN E(I)/E(0) < TOL1
C      TOL2 = TOLERANCE FACTOR THAT STOPS RECURSION AT ORDER N
C      WHEN (E(I)-E(I-1))/E(I-1) < TOL2
C      STATUS = INTEGER INDICATOR OF WHICH OF FIVE CONDITIONS EXISTED
C      AT TIME OF SUBROUTINE EXIT
C      E0 = TOTAL SIGNAL ENERGY
C      PE = ARRAY OF E VALUES J=1 TO M
C      COMPLEX X(1),A(1),C(101),D(101),F,B,M,S,U,U
C      DIMENSION PE(1)
C      INTEGER STATUS
C      C      INITIALIZATION
C      DO 10 K=1,M
C      E0=E0+REAL(X(K))**2+AIMAG(X(K))**2
C      A(1)=E0
C      C=CPLX(018REAL(X(1)),-018AIMAG(X(1)))
C      U=018REAL(X(1))**2+AIMAG(X(1))**2
C      D=018REAL(X(N))**2+AIMAG(X(N))**2
C      DEN=1.-G-U
C      A(1)=DEN
C      S=S+X(NK)
C      F=F+X(1)
C      B=X(N)
C      H=02CONJG(X(N))
C      S=02X(N)
C      U=01X(N)/X(N)
C      V=02CONJG(X(1))
C      E=E+DEN
C      C(1)=018CONJG(X(1))
C      B(1)=01X(N)
C      SAVE1=(0.,0.)
C      NI=NI+1
C      NR=NR+1
C      DO 20 K=1,NR
C      SAVE1=SAVE1+X(K+1)*CONJG(X(K))
C      R(1)=E.SAVE1
C      A(1)=CPLX(-018REAL(R(1)),-018AIMAG(R(1)))
C      E=E+R(1)-REAL(A(1))**2+AIMAG(A(1))**2
C      PE(1)=E
C      IF (M.LT. NMAX) GO TO 40
C      STATUS=1
C      RETURN
C      PREDICTION FILTER ERROR UPDATE
C      EDJ=E
C      FI=FI+1
C      F=X(FI)
C      B=X(NR)
C      DO 50 K=1,M
C      F=F+X(FI-K)*B(K)
C      D=B*X(NR+K)*CONJG(A(K))
C      AUXILIARY VECTOR ORDER UPDATE
C      Q1=1./E
C      Q2=CPLX(018REAL(F),-018AIMAG(F))
C      Q3=CPLX(018REAL(B),018AIMAG(B))
C      DO 80 K=1,-1
C      K1=K+1
C      C(K1)=C(K)+Q2BA(K)
C      D(K1)=D(K)+Q3BA(K)
C      D(1)=Q3
C      SCALAR ORDER UPDATE
C      O7=REAL(S)**2+AIMAG(S)**2
C      Y1=REAL(F)**2+AIMAG(F)**2
C      Y3=REAL(B)**2+AIMAG(B)**2
C      Y2=REAL(U)**2+AIMAG(U)**2
C      Y4=REAL(V)**2+AIMAG(V)**2
C      G=0+Y1*Q1+Q48(Y2*Q6-075*Q5+2.*REAL(CONJG(U))H*H*S)
C      H=0.(0.)
C      S=0.(0.)
C      U=0.(0.)
C      V=0.(0.)
C      DO 70 K=0,M
C      K1=K+1
C      NE=NE-K
C      H=H+CONJG(X(NR+K))B(K)
C      S=S+X(NK)D(K)
C      U=U+X(NK)D(K)
C      V=V+CONJG(X(K))B(K)
C      DENOMINATOR UPDATE
C      O5=1.-G
C      O6=1.-U
C      DEN=O5*O6-REAL(H)**2+AIMAG(H)**2
C      IF (DEN.GT. 0.) GO TO 80
C      STATUS=2
C      RETURN
C      TIME SHIFT VARIABLES UPDATE
C      O4=1./DEN
C      O1=0104
C      ALPHA=1./((1.-Y1*O6+Y3*O5+2.*REAL(H*F*B))H*O1)
C      E=ALPHA*E
C      C1=048(F*O6+CONJG(B)*H)
C      C2=048(CONJG(B)*O5+H*F)
C      C3=048(U*O6+H*S)
C      C4=048(S*O5+U*CONJG(H))
C      C5=048(V*O6+H*U)
C      C6=048(U*O5+V*CONJG(H))
C      DO 90 K=1,N
C      K1=K+1
C      A(K)=ALPHA*A(K)+C1B(K)+C2B(K)+C3B(K)+C4B(K)
C      D(K)=D(K)+C5
C      DO 100 K=1,NE
C      NK=N+2-K
C      SAVE1=CONJG(C(K))
C      SAVE2=CONJG(D(K))
C      SAVE3=CONJG(C(NK))
C      SAVE4=CONJG(D(NK))
C      C(K)=C(K)+C3*SAVE3+C4*SAVE4

```

Figure A-1. Computer program for MSA. (Cont'd)

```

100 B1E)=B1E)+C(S$NAME3)+C(S$NAME4
      IF (.EQ. E) GO TO 106
      C1(R)=C1(R)+C(S$NAME1)+C(S$NAME2
      B1(R)=B1(R)+C(S$NAME1)+C(S$NAME2
      CONTINUE
      GOTO 106
110 GOSUB UPDATE
      R=R+1
      NR=NR+1
      NI=NI+1
      DELTA=10./NR
      C1=CONJG(X(NI)-R)
      C2=X(NI)
      DO 110 K=NR,1,-1
        B1(K)=B1(K)-X(NI)-E)C1-CONJG(X(K))B2
        DELTA=DELTA+R(K+1)B1(K)
        S1=1/(0.,0.)
        DO 120 L=1,NI
          S1=S1+S1*(X(L)+R)B2CONJG(X(K))
          B1)=2./S1
          DELTA=DELTA+R(L)
          S2=CONJG(-REAL(DELTA)/E,-AIMAG(DELTA)/E)
          A1(NI)=S2
          B2=0/2
          DO 130 L=1,NI
            R(L)=X
            S1=CONJG(A(L))
            A1(L)=A1(L)+R(S2CONJG(A(L)))
            IF (.EQ. NI) GO TO 130
            A1(R)=A1(R)+S1
            CONTINUE
            V1=REAL(S2)B2+AIMAG(S2)B2
            E=E*(1.-V1)
            PC(R)=E
            IF (.V1.LT. 1.) GO TO 140
            STATUS=3
            RETURN
            IF (.EQ. E)B2) GO TO 150
            STATUS=4
            RETURN
            IF ((E)D-E) .GE. E)D)T)D) GO TO 30
            STATUS=5
            RETURN
            END

```

Figure A-1. Computer program for MSA. (Cont'd)

SIMULATION VARIABLES

AR CLUTTER COEFF. = 0.27607E+01 -0.38106E+01 0.25555E+01 -0.92306E+00 0.00000E+00
 SRRS= 0.00000
 CRDS= 0.00000
 N= 40 SIGR= 0.00000
 CLTP= 100.66641 MSU= 100.66626
 N= 4 N= 4

POPULATION ALGORITHM N= 4 E(I)= 0.8052E+04 E(R)= 0.2455E+01

SEARCH TERMINATION STATUS

E(R)/E(I).LT.TOL=0.1000E-02

AR COEFFICIENTS

A(1)= -0.279057E+01 0.000000E+00
 A(2)= 0.798422E+01 0.000000E+00
 A(3)= -0.279056E+01 0.000000E+00
 A(4)= 0.977607E+00 0.000000E+00

PRED. ERROR ENERGY - E(J)

0.2879E+04
 0.1121E+03
 0.5078E+02
 0.2495E+01

PEAK SPECTRAL FREQ.= 0.110 KZ

a) MLSA

J=	PRED. ERROR COEFF. - A(I)	POWER - P(I)	MAIPE - FPE(J)	MAIPE - AIC(J)	PARZEN - CAT(J)
1	-0.255632E+01	0.000000E+00	0.4866162E+02	0.171395E+03	-0.195364E-01
2	0.230032E+01	0.000000E+00	0.143048E+01	0.305603E+02	-0.643137E+00
3	-0.160457E+00	0.000000E+00	0.777295E+00	0.502212E+01	-0.114329E+01
4	-0.126270E+01	0.000000E+00	0.353410E-01	-0.116582E+03	-0.240963E+02
5	0.677510E+00	0.000000E+00	0.253918E-01	-0.130933E+03	-0.320325E+02
6	0.808213E+00	0.000000E+00	0.251017E-01	-0.131382E+03	-0.314828E+02
7	-0.978873E+00	0.000000E+00	0.249833E-01	-0.131572E+03	-0.298147E+02
8	0.460419E+00	0.000000E+00	0.197836E-01	-0.140918E+03	-0.362272E+02

PEAK SPECTRAL FREQ.= 0.112 KZ

b) ABA

Figure A-2. Example printouts for AR(4) process.

SIMULATION VARIABLES

A1= 0.10000E+01 F1= 0.72500E+01 PH11= 0.50000E+02
 A2= 0.00000E+00 F2= 0.00000E+00 PH12= 0.00000E+00

SNRDB= 17. SIGPR= 0.50000 NPR= 0.01020
 CNRDB= 0. CLTPR= 0.00000 MSU= 0.51886

N= 101 M= 15 MC= 0

SAMPLE ALGORITHM M=15 E(O)= 0.1048E+03 E(M)= 0.1832E+01

SEARCH TERMINATION STATUS

M=MAX

AR COEFFICIENTS

PRED. ERROR ENERGY - E(J)

A(1)=	-0.2857594E+00	0.0000000E+00	0.2350E+02
A(2)=	-0.1588735E+00	0.0000000E+00	0.7479E+01
A(3)=	-0.1467246E-01	0.0000000E+00	0.4269E+01
A(4)=	0.7109234E-02	0.0000000E+00	0.3291E+01
A(5)=	0.2159619E+00	0.0000000E+00	0.2659E+01
A(6)=	0.8951070E-01	0.0000000E+00	0.2431E+01
A(7)=	0.1274108E+00	0.0000000E+00	0.2324E+01
A(8)=	-0.8820665E-01	0.0000000E+00	0.2295E+01
A(9)=	-0.1214991E+00	0.0000000E+00	0.2276E+01
A(10)=	0.1764777E+00	0.0000000E+00	0.2250E+01
A(11)=	-0.3208539E-01	0.0000000E+00	0.2179E+01
A(12)=	-0.1598348E-01	0.0000000E+00	0.2099E+01
A(13)=	-0.2439793E+00	0.0000000E+00	0.1893E+01
A(14)=	-0.1402914E+00	0.0000000E+00	0.1843E+01
A(15)=	-0.3381020E-01	0.0000000E+00	0.1832E+01

PEAK SPECTRAL FREQ.= 7.250 HZ

a) MLSA

	PRED. ERROR COEFF. - A(J)	POWER - P(J)	AKAIKE - FPE(J)	AKAIKE - AIC(J)	PARZEN - CAT (J)
J= 1	-0.4259099E+00	0.0000000E+00	0.1176132E+00	0.1223652E+00	-0.1861758E+03
J= 2	-0.1838793E+00	0.0000000E+00	0.3802913E-01	0.4035744E-01	-0.3002097E+03
J= 3	0.3256058E-01	0.0000000E+00	0.2189719E-01	0.2370314E-01	-0.3559611E+03
J= 4	0.8009565E-01	0.0000000E+00	0.1732439E-01	0.1912901E-01	-0.3796197E+03
J= 5	0.2411955E+00	0.0000000E+00	0.1432076E-01	0.1612970E-01	-0.3988506E+03
J= 6	0.1203184E+00	0.0000000E+00	0.1337167E-01	0.1536319E-01	-0.4057763E+03
J= 7	0.1248754E+00	0.0000000E+00	0.1301201E-01	0.1525064E-01	-0.4085301E+03
J= 8	-0.8266175E-01	0.0000000E+00	0.1300323E-01	0.1554734E-01	-0.4085983E+03
J= 9	-0.1028400E+00	0.0000000E+00	0.1297513E-01	0.1582681E-01	-0.4088168E+03
J= 10	0.1777890E+00	0.0000000E+00	0.1276656E-01	0.1588727E-01	-0.4104536E+03
J= 11	-0.3314113E-01	0.0000000E+00	0.1263052E-01	0.1603650E-01	-0.4115356E+03
J= 12	0.2440746E-01	0.0000000E+00	0.1257046E-01	0.1628446E-01	-0.4120170E+03
J= 13	-0.1854111E+00	0.0000000E+00	0.1210013E-01	0.1599442E-01	-0.4158685E+03
J= 14	-0.5141038E-01	0.0000000E+00	0.1200554E-01	0.1630143E-01	-0.4159903E+03
J= 15	0.3931342E-01	0.0000000E+00	0.1206686E-01	0.1660968E-01	-0.4161465E+03

PEAK SPECTRAL FREQ.= 7.375 HZ

b) ABA

Figure A-3. Example printouts for noisy sinusoid.

Table A-1. Input Parameters for Program MSA. (Cont'd).

<u>Card</u>	<u>Symbols</u>	<u>Function</u>
	M	Maximum order of AR Prediction used to terminate ABA and possibly MLSA.
	MC	Order of AR test waveform.
	K	Number of points in PSD plot.
6	FN	Sampling frequency (Hz).
	FI, FF	Initial and final frequencies in PSD plot (Hz).
	TOL 1	Ratio of final to initial estimation error in MLSA which if reached will terminate search. (Default = 0.001).
	TOL 2	Ratio of present estimation error to previous order error in MLSA which if reached will terminate search. (Default = 0.005).
7	AR	Array of MC coefficients for AR(MC) test signal (ICLT = 1).

Table A-2. Subroutines for MSA Program.

<u>S. R.</u>	<u>Purpose</u>
SIGI	Generate sinusoidal samples, Eqn. (45).
GASS	Generate Gaussian noise samples with zero mean and standard deviation σ .
NPWR	Calculate sample mean-square-value for signal, noise, and signal plus noise.
FPE1	Calculate three prediction-error estimates (IALG = 0), Eqns. (22) and (23).
MFREQR	Compute PSD, Eqn. (5).
PLT	Generate plot of PSD (dB) vs. Frequency (Hz) and identify frequency location of spectral peak.
MEMC	Complex-data version of ABA. (IALG = 0).
ARCLTR	Generate AR(MC) samples, Eqn. (2).
MARPLE	Marple's least-squares algorithm. (IALG = 1).

Example 1 = AR(4) Model (CNR = 50dB)

This example estimates the PSD for a given AR(4) process with coefficients shown in "AR CLUTTER COEFF. =" line in Figure A-2(a). The Marple algorithm (MLSA) terminated with M=4 (the proper choice) because $E(4)/E(\phi) < 0.001$ as shown. The AR coefficient closely approximate the negatives of the defined values because the minus sign of Eqn. (2) was inadvertently omitted from S.R. ARCLTR. This could readily be corrected by the change

$$XC(J) = \text{CMLPX} (-X(K), \phi . \phi) .$$

The ABA was permitted to run to M=8 to show the three predictor-order results. Using first minimum choices, the proper order would be FPE=5, $AIC \geq 8$ (with a rather flat value for $5 \leq M \leq 7$), and CAT=5. The PSD plot appears in Figure A-4.

Example 2 - Noisy Sinusoid (SNR = 17 dB)

The second example is for a noisy sinusoid described by Eqn. (41). The user supplies the SNR (17 dB) which is converted to a number from which σ (SIGMA) can be determined in accord with Eqn. (42). Note that the second signal amplitude (A2) must be set equal to zero as shown in Figure A-3(a). In this case the prediction order reaches the preset maximum (MMAX) of 15. The ABA predictors shown in Figure A-3(b) indicate FPE=7, $AIC \geq 15$ (with flat values in the ranges $7 \leq M \leq 9$ and $13 \leq M \leq 15$), and CAT=7. The spectral frequency for ABA is 7.375 Hz vs. the correct MLSA estimate of 7.250 Hz. The ABA spectral estimate shown in Figure A-4 also has considerably more sidelobe energy over the region dc to $1/4T$.

Generating data samples for a pair of sinusoids simply requires supplying non-zero values for the three parameters of Card 4 in Table A-1. The user-supplied SNR is based on the formula

$$\alpha = (A_1^2 + A_2^2) / 2\sigma^2$$

and is used for both real and complex valued signals. Results of such simulations are recorded in Section IV. C.

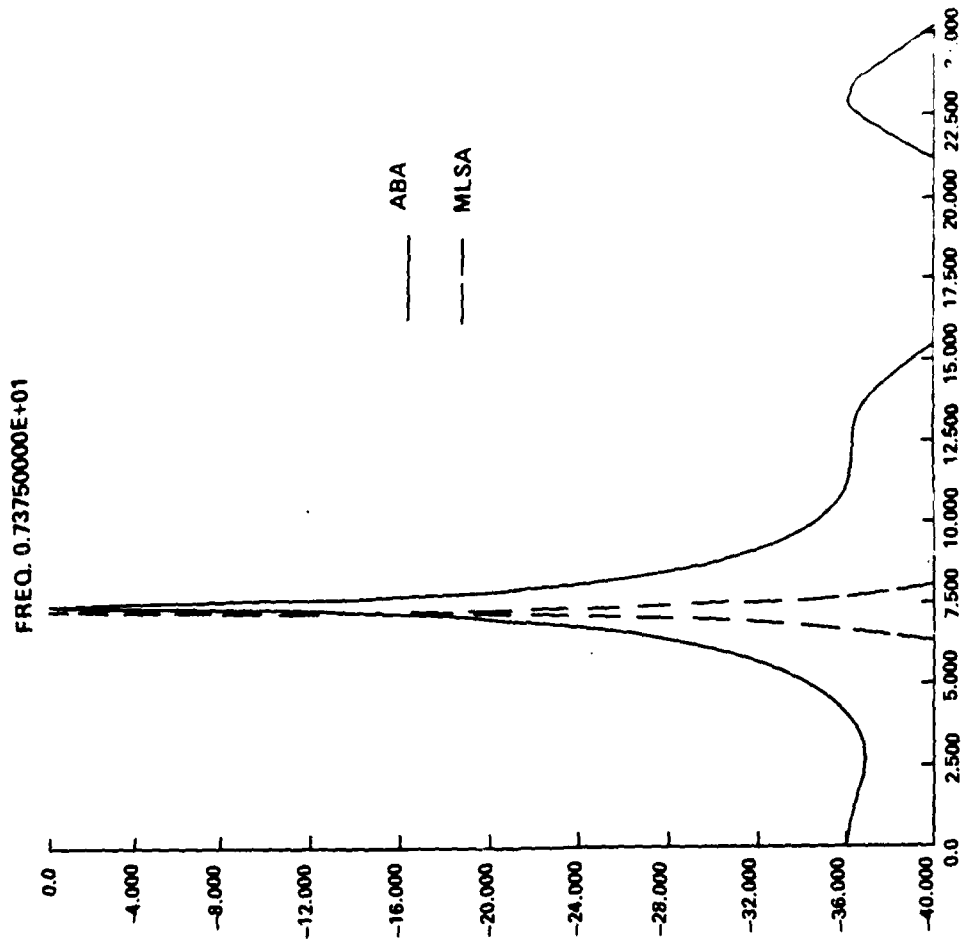


Figure A-4. PSD plots for noisy sinusoid.

DISTRIBUTION

	<u>Copies</u>
US Army Materiel Systems Analysis Activity ATTN: AMXSY-MP Aberdeen Proving Ground, MD 21005	1
AMSMI-R, Dr. McCorkle	1
Dr. Rhoades	1
-RER	5
-LP, Mr. Voigt	1
-RPR	15
-RPT	1

END

FILMED

6-85

DTIC